A Distributed, Event-triggered, Adaptive Controller for Cooperative Manipulation with Rolling Contacts

Wenceslao Shaw Cortez, Christos K. Verginis, and Dimos V. Dimarogonas

***Abstract*—We present a distributed, event-triggered, and adaptive control algorithm for cooperative object manipulation with rolling contacts and unknown dynamic parameters. Whereas conventional cooperative manipulation methods require rigid contact points, our approach exploits rolling effects of passive end-effectors and does not require force/torque sensing. The removal of rigidity allows for more modular grasping, increased application to more object types, and online adjustment of the grasp. The proposed control algorithm exhibits the following properties. Firstly, it is distributed, in the sense that the robotic agents calculate their own control signal, under an event-triggered communication scheme. Such a scheme reduces the inter-agent communication requirements with respect to continuous communication schemes. Secondly, it uses an online adaptation mechanism to accommodate for unknown dynamic parameters of the object and the agents. Finally, it adapts existing internal force controllers to guarantee no slip throughout the manipulation task despite the event-triggered nature of the communication scheme. Hardware implementation validates the effectiveness of the proposed approach.**

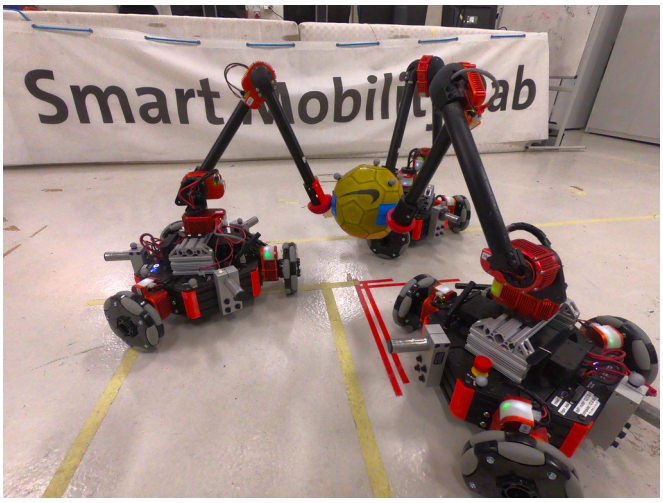

Fig. 1: Non-rigid grasping of object with mobile manipulators.

Fig. 2: Objects (from left to right): hex, ball, and box.

I. Introduction

Recent technological advancements have led to the concept of automated manufacturing where the ability to transport objects/packages autonomously is key to the production process. One popular, modular approach to perform object transport is via cooperative manipulation, which entails the transport/manipulation of an object by using multiple mobile manipulators. Due to the different objects that must be transported in such a setting, the cooperative manipulation methods should be robust to uncertainties in object weight, inertia, shape, and even center of mass location.

Existing methods in cooperative manipulation aim to track a desired object reference trajectory using robotic manipulators on mobile bases. Multiple robots allow for carrying heavy loads and executing dexterous maneuvers. Early works in cooperative manipulation focused on hybrid force/position and impedance control schemes [1], [2]. Other approaches focused on decentralization of the agents [3] and adaptive controllers [4], [5]. However, those methods rely on the assumption that each agent is *rigidly* fixed to the object, allowing it to apply any force/torque at the contact point. The rigidity assumption is highly restrictive as it only applies to objects on which a rigid grasp can be formed, excluding, e.g., objects with smooth surfaces or large boxes/spheres (e.g packages), which cannot be rigidly grasped by a simple gripper. Furthermore, many existing approaches are dependent on force/torque sensors mounted on each robot, which can be expensive or difficult to equip appropriately on a fleet of mobile manipulators.

We aim to remove the rigidity assumption that is characteristic of current cooperative manipulation approaches, and relax the dependency on tactile sensors to contact location sensors only by exploiting the natural rolling of a passive end-effector. Non-rigid/rolling contacts increase the number of objects that can be grasped, increase the workspace of the system, and allow for scenarios in which robots can be swapped in/out to adjust the grasp online. Note that by employing rolling contacts, the cooperative manipulation problem here is similar to robotic grasping [6] albeit with mobile "fingers." An example of non-rigid grasping is shown in Figure 1.

Despite advancements in the literature, existing methods from cooperative manipulation and robotic grasping are not applicable to the cooperative manipulation problem posed here due to their dependence on rigid grasps, known dynamics, and/or centralized schemes. The aforementioned works in

This work was supported by the Swedish Research Council (VR), the H2020 ERC Consolidator Grant LEAFHOUND, the Knut and Alice Wallenberg Foundation (KAW), and the H2020-EU Research and Innovation Programme under the GA No. 101016906 (CANOPIES).
W. Shaw Cortez is with the Pacific Northwest National Laboratory, Richland, WA, USA (w.shawcortez@pnnl.gov). C. K. Verginis is with the Division of Signals and Systems, Department of Electrical Engineering, Uppsala University, Uppsala, Sweden (christos.verginis@angstrom.uu.se). D. V. Dimarogonas is with the School of Electrical Engineering, KTH Royal Institute of Technology, Sweden (dimos@kth.se).

cooperative manipulation [1]–[5] are not applicable due to the dependency on rigid contacts. Rolling contacts complicate the problem as each contact may only apply a force that respects friction cone constraints to prevent slip, instead of an arbitrary wrench associated with rigid contacts [7]. Early robotic grasping approaches required exact knowledge of the agent's dynamics [7], [8]. Other recent techniques are robust to model uncertainties, but neglect rolling effects or dynamics [9]–[11], while other more sensor-deprived approaches assume the object is weightless [12], [13]. The approach from [14] assumes a priori bounded states, which does not apply to the mobile manipulators considered here. Adaptive control schemes that have also been developed require force *and* contact location sensing, and assume boundedness of the uncertain parameter estimates [15], [16], or are limited to set-point (constant reference) manipulation [17]. Additionally, all robotic grasping methods are formulated as centralized controllers, which would require large communication requirements between all agents. Such centralized approaches do not scale well with the number of agents and are highly sensitive to faults of the central controller. Finally, most related works (e.g., [1], [4], [5], [8]) consider accurate knowledge of the object center of mass, which can be difficult to obtain in practice, especially in cases of complicated object shapes. Thus, there exists no distributed, robust cooperative manipulation approach that ensures stability to a reference trajectory with non-rigid, rolling contacts and no force/torque sensing.

A critical attribute of cooperative manipulation with rolling contacts is that of object slip. The agents need to exert the appropriate forces in order to maintain contact with the object and avoid slip without jeopardizing the manipulation task. Methods of ensuring slip prevention are developed typically by solving an optimization problem online [9], [18], [19]. However [9], [19] neglect the agent dynamics, which may perturb the system and cause slip. The approach in [18] is centralized and would require a central computer unit to compute and distribute to the agents the forces to be applied.

In this paper, we present a novel event-triggered, adaptive control algorithm for the cooperative object manipulation with rolling contacts and unknown dynamic parameters. The algorithm extends the method from [20] in a distributed manner in which each agent calculates its own control signal and determines when inter-agent communication is required independently of other agents. Such a scheme reduces the communication requirements with respect to continuous communication. Moreover, an online adaptation mechanism compensates for the unknown dynamic parameters of the object and the agents. We further adapt existing internal force controllers to our event-triggered scheme that guarantee no slip during the manipulation motion. Hardware implementation is used to validate the proposed approach.

Notation: The notation $\boldsymbol{v}^{\mathcal{E}}$ indicates that the vector $\boldsymbol{v}$ is written with respect to a frame $\mathcal{E}$, and if no explicit frame is defined, $\boldsymbol{v}$ is written with respect to an inertial frame, $\mathcal{P}$. The operator $(\cdot)\times$ denotes the skew-symmetric matrix representation of the cross-product. $SO(3)$ is the special orthogonal group of dimension 3, and S^n is the unit $(n-1)$-dimensional sphere. The $r \times r$ identity matrix is denoted by $I_{r\times r}$ and the r-dimensional vector of zeros by $\mathbf{0}_r$. For a set $\mathcal{B}$, the boundary of $\mathcal{B}$ is denoted $\partial\mathcal{B}$. The terms $\succeq, \preceq$ denote element-wise vector inequalities. The null space of a matrix B is $\mathfrak{N}(B)$, and the interior of a set $\mathcal{A}$ is $\text{Int}(\mathcal{A})$. A continuous function $\alpha : \mathbb{R}_{\geq 0} \to \mathbb{R}_{\geq 0}$ is a class-$\mathcal{K}$ function if it is strictly increasing and $\alpha(0) = 0$. A continuous function $\beta : \mathbb{R}_{\geq 0} \times \mathbb{R}_{\geq 0} \to \mathbb{R}_{\geq 0}$ is a class-$\mathcal{KL}$ function if for each fixed s, $\beta(r, s)$ is a class-$\mathcal{K}$ function, and for each fixed r, $\beta(r, s)$ is decreasing with respect to s and $\beta(r, s) \to 0$ as $s \to \infty$. The terms $\wedge$ and $\vee$ denote the logical 'and' and 'or' operators, respectively.

II. Problem Formulation

Consider $N \in \mathbb{N}$ robotic agents, consisting of a holonomic moving base and a robotic arm, grasping a rigid object in 3D space. Let their generalized joint space variables and respective derivatives be $\boldsymbol{q}_i, \dot{\boldsymbol{q}}_i \in \mathbb{R}^{n_i}$ with $n_i \geq 3$, for all $i \in \mathcal{N} := \{1, ..., N\}$. Here $\boldsymbol{q}_i$ consists of the degrees of freedom of the robotic arm as well as the moving base. The overall joint configuration is then $\boldsymbol{q} := [\boldsymbol{q}_1^\top, ..., \boldsymbol{q}_N^\top]^\top$, $\dot{\boldsymbol{q}} := [\dot{\boldsymbol{q}}_1^\top, ..., \dot{\boldsymbol{q}}_N^\top]^\top \in \mathbb{R}^n$ with $n := \sum_{i\in\mathcal{N}} n_i$. Each agent has a smooth, convex "fingertip" (i.e. passive end-effector) of high stiffness that is in contact with an object via a smooth contact surface. Let the inertial frame be denoted by $\mathcal{P}$, and an end-effector frame, $\mathcal{F}_i$, fixed at the point $\boldsymbol{p}_{f_i} \in \mathbb{R}^3$ on each end-effector. The rotation matrix from $\mathcal{F}_i$ to $\mathcal{P}$ is $R_{pf_i} := R_{pf_i}(\boldsymbol{q}_i) \in SO(3)$. The contact frame, $\mathcal{C}_i$, is located at the contact point, $\boldsymbol{p}_{c_i} \in \mathbb{R}^3$ and defined as a Gauss frame [21] where one of the axes is defined to be orthonormal to the contact plane. We use the standard assumption that the end-effector surface is smooth and the Gauss frame is well-defined for all points on the surface. The vector from $\mathcal{F}_i$ to $\mathcal{C}_i$ is $\boldsymbol{p}_{fc_i} := \boldsymbol{p}_{c_i} - \boldsymbol{p}_{f_i} \in \mathbb{R}^3$, and $R_{pc_i} = R_{pc_i}(\boldsymbol{p}_{fc_i}, \boldsymbol{q}_i) \in SO(3)$ are the rotation matrices mapping the contact frames $\mathcal{C}_i$ to the inertial frame $\mathcal{P}$. The contact geometry for the ith agent is shown in Figure 3.

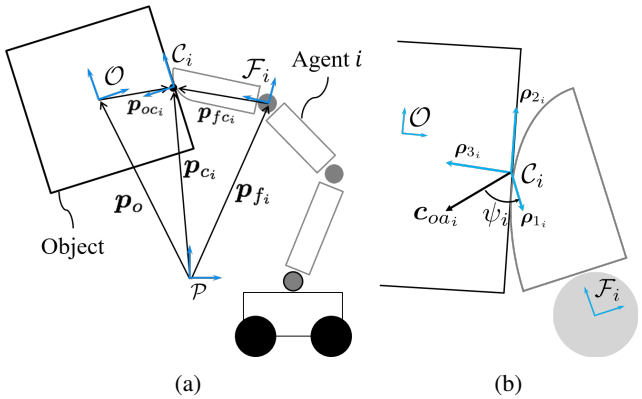

Fig. 3: Object/agent and contact frames for agent i.

The dynamics of agent i is defined by [21]:

$$M_i\ddot{\boldsymbol{q}}_i + C_i\dot{\boldsymbol{q}}_i + \boldsymbol{g}_i = -J_{h_i}^\top \boldsymbol{f}_{c_i} + \boldsymbol{u}_i \tag{1}$$

where $M_i := M_i(\boldsymbol{q}_i) \in \mathbb{R}^{n_i\times n_i}$ is the positive definite inertia matrix, $C_i := C_i(\boldsymbol{q}_i, \dot{\boldsymbol{q}}_i) \in \mathbb{R}^{n_i\times n_i}$ is the Coriolis/centrifugal matrix, $\boldsymbol{g}_i := \boldsymbol{g}_i(\boldsymbol{q}_i) \in \mathbb{R}^{n_i}$ is the gravity torque, $\boldsymbol{f}_{c_i} \in \mathbb{R}^3$ is the contact force exerted at $\boldsymbol{p}_{c_i}$, $\boldsymbol{u}_i \in \mathbb{R}^{n_i}$ is the joint

torque control input; $J_{h_i} := J_{h_i}(\boldsymbol{q}_i, \boldsymbol{p}_{fc_i}) \in \mathbb{R}^{3\times n_i}$ is the agent Jacobian matrix, defined by

$$J_{h_i}(\boldsymbol{q}_i, \boldsymbol{p}_{fc_i}) := \begin{bmatrix} I_3 & -(\boldsymbol{p}_{fc_i})\times \end{bmatrix} J_{s_i}(\boldsymbol{q}_i),$$

where $J_{s_i}(\boldsymbol{q}_i) \in \mathbb{R}^{6\times n_i}$ is the manipulator Jacobian that maps $\dot{\boldsymbol{q}}_i$ to the translational and rotational velocities of $\mathcal{F}_i$ [21]. The full hand Jacobian matrix is $J_h := \text{diag}\{[J_{h_i}]_{i\in\mathcal{N}}\} \in \mathbb{R}^{3N\times n}$. We emphasize that the dynamical parameters, which refer to masses, moments of inertia, and center of mass of the robotic base/links appearing in the terms M_i, C_i, $\boldsymbol{g}_i$, $i \in \mathcal{N}$, are considered to be *unknown*. However, the *kinematic* parameters in J_h, which refer to the link lengths, are assumed known since they can be easily measured. The dynamics (1) can be written in vector form as

$$M\ddot{\boldsymbol{q}} + C\dot{\boldsymbol{q}} + \boldsymbol{g} = -J_h^\top \boldsymbol{f}_c + \boldsymbol{u}, \tag{2}$$

where $M := M(\boldsymbol{q}) := \text{diag}\{[M_i]_{i\in\mathcal{N}}\}$, $C := C(\boldsymbol{q}, \dot{\boldsymbol{q}}) := \text{diag}\{[C_i]_{i\in\mathcal{N}}\} \in \mathbb{R}^{n\times n}$, and $\boldsymbol{g} := \boldsymbol{g}(\boldsymbol{q}) := [\boldsymbol{g}_1^\top, \dots, \boldsymbol{g}_N^\top]^\top$, $\boldsymbol{f}_c := [\boldsymbol{f}_{c_1}^\top, \dots, \boldsymbol{f}_{c_N}^\top]^\top$, $\boldsymbol{u} := [\boldsymbol{u}_1^\top, \dots, \boldsymbol{u}_N^\top]^\top \in \mathbb{R}^n$.

Let $\mathcal{O}$ be a reference frame fixed at $\boldsymbol{p}_o$, which does not need to be coincident with the object center of mass. Let also $R_{po} \in SO(3)$ be the respective rotation matrix, which maps from $\mathcal{O}$ to $\mathcal{P}$. Let $\boldsymbol{x}_o := [\boldsymbol{p}_o^\top, \boldsymbol{\eta}_o^\top]^\top \in \mathbb{M} := \mathbb{R}^3 \times \mathsf{S}^3$, $\boldsymbol{v}_o := [\dot{\boldsymbol{p}}_o^\top, \boldsymbol{\omega}_o^\top]^\top \in \mathbb{R}^6$ denote the pose and generalized velocity of the object frame, with $\boldsymbol{\eta}_o \in \mathsf{S}^3$ as the unit quaternion. The position vector from $\mathcal{O}$ to the respective contact point is $\boldsymbol{p}_{oc_i} := \boldsymbol{p}_{c_i} - \boldsymbol{p}_o \in \mathbb{R}^3$. The assumption is that the system used to track the object is broadcasting $\boldsymbol{x}_o$ and $\dot{\boldsymbol{x}}_o$ to all agents, which is a common assumption in related literature [1], [7], [9], [10], [22]. This assumption can be relaxed by equipping each agent with vision capabilities [23].

We denote by $\bar{\boldsymbol{p}}_o \in \mathbb{R}^3$ the location of the center of mass of the object and, without loss of generality, we align the object body frame with $\mathcal{O}$ so that $\boldsymbol{\eta}_o = \bar{\boldsymbol{\eta}}_o$ and $\bar{\boldsymbol{\omega}}_o = \boldsymbol{\omega}_o$. Thus, we let $\bar{\boldsymbol{x}}_o := [\bar{\boldsymbol{p}}_o^\top, \boldsymbol{\eta}_o^\top]^\top \in \mathbb{M}$ be the object pose with respect to the inertial frame $\mathcal{P}$ and $\bar{\boldsymbol{v}}_o := [\dot{\bar{\boldsymbol{p}}}_o^\top, \boldsymbol{\omega}_o^\top]^\top \in \mathbb{R}^6$. Let $\bar{\boldsymbol{p}}_{oc_i} := \boldsymbol{p}_{c_i} - \bar{\boldsymbol{p}}_o$ with $\boldsymbol{p}_{oc} := [\boldsymbol{p}_{oc_1}^\top, ..., \boldsymbol{p}_{oc_N}^\top]^\top \in \mathbb{R}^{3N}$. The conventional object dynamics with respect to the object center of mass are given by the Newton-Euler formulation:

$$\bar{M}_o\dot{\bar{\boldsymbol{v}}}_o + \bar{C}_o\bar{\boldsymbol{v}}_o + \bar{\boldsymbol{g}}_o = \bar{G}\boldsymbol{f}_c \tag{3}$$

where $\bar{M}_o := \bar{M}_o(\bar{\boldsymbol{\eta}}_o) \in \mathbb{R}^{6\times 6}$ is the object inertia matrix, $\bar{C}_o := \bar{C}_o(\bar{\boldsymbol{\eta}}_o, \bar{\boldsymbol{\omega}}_o) \in \mathbb{R}^{6\times 6}$ is the object Coriolis and centrifugal matrices, $\bar{G} := \bar{G}(\bar{\boldsymbol{p}}_{oc}) \in \mathbb{R}^{6\times 3N}$ is the grasp map, and $\bar{\boldsymbol{g}}_o \in \mathbb{R}^6$ is the gravity acting on the object. Similarly to the agents, the object dynamic parameters, which refer to the object mass, moment of inertia, and center of mass, appearing in the terms M_o, C_o, $\boldsymbol{g}_o$ are considered to be *unknown*.

The grasp map, $\bar{G}$, maps the concatenated contact force, $\boldsymbol{f}_c \in \mathbb{R}^{3N}$, to the net wrench acting on the object *center of mass* and is defined by $\bar{G} := [\bar{G}_1, ..., \bar{G}_N]$ where $\bar{G}_i := \bar{G}_i(\bar{\boldsymbol{p}}_{oc_i}) := [I_3, -(\bar{\boldsymbol{p}}_{oc_i})\times]^\top \in \mathbb{R}^{6\times 3}$. We note that $\bar{G}$ is the conventional grasp map commonly used in grasping [21].

Regarding the object orientation, we use the unit quaternion choice $\boldsymbol{\eta}_o := [\varphi_o, \boldsymbol{\epsilon}_o^\top]^\top$, where $\varphi_o \in [-1, 1]$ and $\boldsymbol{\epsilon}_o \in \mathbb{R}^3$ are the scalar and vector part, respectively, satisfying $\varphi_o^2 + \boldsymbol{\epsilon}_o^\top\boldsymbol{\epsilon}_o = 1$. Moreover, it holds that [5]

$$\dot{\boldsymbol{\eta}}_o = \frac{1}{2}E_\eta(\boldsymbol{\eta}_o)\boldsymbol{\omega}_o \Rightarrow \boldsymbol{\omega}_o = 2E_\eta(\boldsymbol{\eta}_o)^\top\dot{\boldsymbol{\eta}}_o, \tag{4}$$

where $E_\eta : \mathsf{S}^3 \to \mathbb{R}^{4\times 3}$ is the matrix

$$E_\eta(\boldsymbol{\eta}) := \begin{bmatrix} -\boldsymbol{\epsilon}^\top \\ \varphi I_3 - (\boldsymbol{\epsilon})\times \end{bmatrix}, \quad \forall \boldsymbol{\eta} = [\varphi, \boldsymbol{\epsilon}^\top]^\top \in \mathsf{S}^3.$$

The more practical consideration of rolling contacts, as opposed to a rigid grasp, requires no slip to occur between the agents and object by ensuring that each contact force remains inside the friction cone defined by [21]:

$$\mathcal{F}_{c_i}(\mu) := \{\boldsymbol{f}_{c_i}^{\mathcal{C}_i} \in \mathbb{R}^3 : f_{n_i}\mu \geq \sqrt{f_{x_i}^2 + f_{y_i}^2}\} \tag{5}$$

where $\boldsymbol{f}_{c_i}^{\mathcal{C}_i} = (f_{x_i}, f_{y_i}, f_{n_i})$ is the contact force at i written in frame $\mathcal{C}_i$ with tangential force components $f_{x_i}, f_{y_i} \in \mathbb{R}$ and normal force component $f_{n_i} \in \mathbb{R}$, and $\mu \in \mathbb{R}_{>0}$ is the friction coefficient. The full friction cone is the Cartesian product of all the friction cones: $\mathcal{F}_c := \mathcal{F}_{c_1} \times ... \times \mathcal{F}_{c_n}$.

Let now a desired pose trajectory, $\boldsymbol{p}_\text{d} : \mathbb{R}_{\geq 0} \to \mathbb{R}^3$, $\boldsymbol{\eta}_\text{d} := [\varphi_\text{d}, \epsilon_\text{d}^\top]^\top : \mathbb{R}_{\geq 0} \to \mathsf{S}^3$, to be tracked by $\boldsymbol{x}_o$. To that end, we define the position error $\boldsymbol{e}_p := \boldsymbol{p}_o - \boldsymbol{p}_\text{d}$ as well as the quaternion product $\boldsymbol{e}_\eta := \boldsymbol{\eta}_\text{d} \otimes \boldsymbol{\eta}_o^+$, as an orientation error metric [5], where $\boldsymbol{\eta}^+ := [\varphi, -\boldsymbol{\epsilon}^\top]^\top$ denotes the quaternion conjugate. The aim is then to regulate $\boldsymbol{e}_\eta$ to $[\pm 1, \boldsymbol{0}_3^\top]^\top$ [5]. Moreover, we aim at ensuring that the end-effectors are always in contact with the object and slipping is avoided. Formally, the problem is defined as follows.

Problem 1. *Given a desired bounded, smooth object pose trajectory defined by $\boldsymbol{p}_d : \mathbb{R}_{\geq 0} \to \mathbb{R}^3$, $\boldsymbol{\eta}_d : \mathbb{R}_{\geq 0} \to \mathsf{S}^3$, with bounded first and second derivatives, determine a distributed control law $\boldsymbol{u}$ in* (2) *such that the following conditions hold:*

1) $lim_{t\to\infty}\big(\boldsymbol{e}_p(t), \boldsymbol{e}_\eta(t)\big) = \big(\boldsymbol{0}_3, [\pm 1, \boldsymbol{0}_3^\top]^\top\big)$
2) $\boldsymbol{f}_{c_i}^{C_i}(t) \in \mathcal{F}_{c_i}, \forall t \geq 0,\ i \in \mathcal{N}$.

III. Proposed Solution

This section presents the proposed control algorithm, which exhibits the following properties: first, it is distributed, in the sense that each agent calculates its own control signal and determines when an event (inter-agent communication) is needed; second, it employs an even-triggered communication scheme to reduce the communication requirements of the agents; third, it employs adaptive control techniques for the compensation of the dynamic uncertainties of the agent and object; fourth, it guarantees avoidance of object slip through the appropriate design of internal forces.

We organize the presentation of the proposed solution's components as follows. First, we present a rigid body transformation used to handle the unknown object center of mass. Second, we introduce an internal-force algorithm that ensures slip avoidance and thus allows for rolling contacts. Third, we use the rolling contact kinematics to determine the coupled agent-object dynamics and formulate an adaptive control law that compensates for the uncertain dynamic parameters of both the agents and the object. Fourth, we introduce the event-triggering update law that dictates the time instants that the agents communicate with each other. Finally, we prove the stability of the closed-loop system and discuss the implementation of the proposed algorithm.

As stated, the proposed controller relies on an event-triggered methodology, wherein many different components of the control will be updated at each event. Thus, we introduce first the event-triggering elements. At each event, the *only* updated terms are $\boldsymbol{p}_{oc_i}$ and the quaternion representation of R_{pc_i}, which we denote $\boldsymbol{\eta}_{pc_i}$, between all agents, at each time $t_k \in \mathbb{R}_{>0}$ for $k \in \mathbb{N}$. We use the subscript k to denote a variable that is held constant over the time interval $[t_k, t_{k+1})$ and updated at each t_{k+1}. For example, $\boldsymbol{\eta}_{pc_{k,i}} = \boldsymbol{\eta}_{pc_i}(t = t_k)$, $R_{pc_{k,i}} = R_{pc_i}(t = t_k)$, $\boldsymbol{p}_{oc_{k,i}} = \boldsymbol{p}_{oc_i}(t = t_k)$. All agents broadcast such information at t_k so that all agents have access to $R_{pc_{k,i}}$, $p_{oc_{k,i}}$ for all $i \in \mathcal{N}$. The events are defined based on how much $R_{pc_{k,i}}$ and $\boldsymbol{p}_{oc_{k,i}}$ deviate from their true values, which will impact stability and slip prevention.

The main variables used in the proposed approach can be found in Table I.

TABLE I: Table of Variables

Variable	Description
$\mathcal{C}_i$	Frame fixed to contact i.
$C_i, C_o, \tilde{C}$	Coriolis matrix of agent i, the object, and the agent-object system, resp.
$\delta_p, \delta_r, \delta_c$	Event-triggering parameters.
$\Delta\boldsymbol{p}_{oc_i}$	Error in $\boldsymbol{p}_{oc_i}$ and $\boldsymbol{p}_{oc_{k,i}}$.
$\varepsilon, \varepsilon_c$	Design parameters for the internal force controller and event triggering, resp.
$\boldsymbol{e}$	Pose error of the object.
$\boldsymbol{e}_\epsilon, e_\varphi$	Quaternion components of $\boldsymbol{e}_\eta$.
$\boldsymbol{e}_p, \boldsymbol{e}_\eta$	Error between true and desired vectors for the object position and orientation, resp.
$\boldsymbol{e}_\nu, \boldsymbol{e}_{\nu_o}$	Error in estimated dynamic parameters and true dynamic parameters w.r.t the agents and object, resp.
$\boldsymbol{e}_v$	Error between $\boldsymbol{v}_o$ and $\boldsymbol{v}_f$.
$\boldsymbol{\eta}_{pc}, \boldsymbol{\eta}_o, \boldsymbol{\eta}_d$	Quaternion representation of R_{pc}, R_{po}, and the desired orientation, resp.
$\boldsymbol{f}_{c_i}$	Contact force of agent i.
$\mathcal{F}_i$	Frame fixed to agent i's end-effector.
$\mathcal{F}_{c_i}, \mathring{\mathcal{F}}_{c_i}$	Friction cone, friction pyramid, resp.
$\boldsymbol{f}_{\text{int}_k}$	Internal force controller written in the inertial frame.
G_i	Grasp map for agent i.
$\boldsymbol{g}_i, \boldsymbol{g}_o, \tilde{\boldsymbol{g}}$	Gravity vector of agent i, the object, and the agent-object system, resp.
γ	Event-triggering parameter.
Γ, Γ_o	Gain matrices for the adaptive control associated with the agents and object, resp.
J_{h_i}	Agent manipulation Jacobian.
$\boldsymbol{\ell}_k^*$	Internal force controller with elements written in the respective contact frames.
Λ_i	Matrix used to define the friction pyramid.
$\boldsymbol{\lambda}_{k_i}$	Manipulation force controller.
μ	Friction coefficient.
$M_i, M_o, \tilde{M}$	Inertia matrix of agent i, the object, and the agent-object system, resp.
$\boldsymbol{\nu}_i, \boldsymbol{\nu}_o$	Dynamic parameters of agent i and the object, resp.
$\hat{\boldsymbol{\nu}}_i, \hat{\boldsymbol{\nu}}_o$	Estimates of $\boldsymbol{\nu}_i, \boldsymbol{\nu}_o$ resp.
$\mathcal{O}$	Frame fixed to the object.
$\mathcal{P}$	Inertial frame.
$\boldsymbol{p}_o, \boldsymbol{p}_d$	Position of $\mathcal{O}$ and desired position, resp.
$\boldsymbol{p}_{fc_i}, \boldsymbol{p}_{oc_i}$	Vectors to contact i from agent i's end-effector and the object, resp.
$\boldsymbol{q}_i$	Joint configuration of agent i.
R_{pc_i}, R_{po}	Rotation matrix from inertial frame to $\mathcal{C}_i$ and $\mathcal{O}$, resp.
$\boldsymbol{u}_i$	Control torque of agent i.
$\boldsymbol{v}_o, \boldsymbol{v}_d$	Translational and angular velocity of the object and desired trajectory, resp.
$\boldsymbol{v}_f$	Reference velocity term.
Y_i, Y_o	Regressor matrix of agent i and the object, resp.
Y_{r_i}, Y_{o_r}	Reference versions of Y_i, Y_o, resp.

A. Handling the Uncertain Object Center of Mass

A common assumption in the majority of the works in the related literature is that the object center of mass is accurately known (e.g., [1], [4], [5], [8]), which is typically not the case in practice. In this work, we assume tracking of a traceable point $\boldsymbol{p}_o$ on the object surface instead of the center of mass, whose information is considered unknown. Note that appropriate sensor equipment, e.g., cameras and markers, can accurately track such points in practice. Hence, to remove the dependency on an unknown object center of mass, we perform a standard rigid body transformation to the conventional object dynamics as follows. To perform the rigid body transformation, let $J_a \coloneqq J_a(\bar{\boldsymbol{\eta}}_o) \in \mathbb{R}^{6\times 6}$ be defined as:

$$J_a(\bar{\boldsymbol{\eta}}_o) \coloneqq \begin{bmatrix} I_3 & (R_{po}\boldsymbol{p}_{\bar{o}o}^{\mathcal{O}})\times \\ \mathbf{0}_3 & I_3 \end{bmatrix} \tag{6}$$

where $\boldsymbol{p}_{\bar{o}o}^{\mathcal{O}} \coloneqq \boldsymbol{p}_o^{\mathcal{O}} - \bar{\boldsymbol{p}}_o^{\mathcal{O}}$, such that $\bar{\boldsymbol{v}}_o$ and $\boldsymbol{v}_o$ can be related via $\bar{\boldsymbol{v}}_o = J_a\boldsymbol{v}_o$, which is derived by differentiating $\bar{\boldsymbol{p}}_o = \boldsymbol{p}_o + R_{po}(\bar{\boldsymbol{p}}_o^{\mathcal{O}} - \boldsymbol{p}_o^{\mathcal{O}})$. Note that $\boldsymbol{p}_{\bar{o}o}^{\mathcal{O}}$ is constant.

Substitution of $\bar{\boldsymbol{v}}_o = J_a\boldsymbol{v}_o$ and left multiplication by $J_a^\top$ in (3) yields the adjusted object dynamics with respect to $\boldsymbol{p}_o$:

$$M_o\dot{\boldsymbol{v}}_o + C_o\boldsymbol{v}_o + \boldsymbol{g}_o = G\boldsymbol{f}_c, \tag{7}$$

where $M_o \coloneqq M_o(\bar{\boldsymbol{\eta}}_o) \coloneqq J_a^\top \bar{M}_o J_a \in \mathbb{R}^{6\times 6}$, $C_o \coloneqq C_o(\bar{\boldsymbol{\eta}}_o, \boldsymbol{\omega}_o) \coloneqq J_a^\top(\bar{M}_o\dot{J}_a + \bar{C}_o J_a) \in \mathbb{R}^{6\times 6}$, $\boldsymbol{g}_o \coloneqq \boldsymbol{g}_o(\bar{\boldsymbol{\eta}}_o) \coloneqq J_a^\top \bar{\boldsymbol{g}}_o \in \mathbb{R}^6$, and $G \coloneqq J_a^\top \bar{G} \in \mathbb{R}^{6\times 6}$, for which it holds $G = [G_1, \ldots, G_N]$, with

$$G_i = J_a^\top \bar{G}_i = \begin{bmatrix} I_3 \\ -(R_{po}\boldsymbol{p}_{\bar{o}o}^{\mathcal{O}})\times + (\bar{\boldsymbol{p}}_{oc_i})\times \end{bmatrix} = \begin{bmatrix} I_3 \\ (\boldsymbol{p}_{oc_i})\times \end{bmatrix},$$

where we have used $R_{po}\bar{\boldsymbol{p}}_{\bar{o}o}^{\mathcal{O}} = \boldsymbol{p}_{\bar{o}o}$ such that $-\boldsymbol{p}_{\bar{o}o} + \bar{\boldsymbol{p}}_{oc_i} = \boldsymbol{p}_{oc_i}$. Note that $G = G(\boldsymbol{p}_{oc})$, i.e., G is *not* dependent on $\bar{\boldsymbol{p}}_o$. Note also by the relation $\bar{\boldsymbol{p}}_o = \boldsymbol{p}_o - R_{po}\boldsymbol{p}_{\bar{o}o}^{\mathcal{O}}$ that M_o, C_o, $\boldsymbol{g}_o$ are functions of $\bar{\boldsymbol{\eta}}_o = \boldsymbol{\eta}_o$, $\bar{\boldsymbol{\omega}}_o = \boldsymbol{\omega}_o$ with dependency on the

constant but unknown term $\boldsymbol{p}_{\bar{o}o}^{\mathcal{O}}$. We also note the following relation that will be needed subsequently:

$$\bar{G}_i^\top \bar{\boldsymbol{v}}_o = \begin{bmatrix} I_3 \\ (\boldsymbol{p}_{c_i} - \bar{\boldsymbol{p}}_o)\times \end{bmatrix}^\top \begin{bmatrix} I_3 & (R_{po}\boldsymbol{p}_{\bar{o}o}^{\mathcal{O}})\times \\ \mathbf{0}_3 & I_3 \end{bmatrix} \boldsymbol{v}_o = G_i^\top \boldsymbol{v}_o \tag{8}$$

B. No Slip Control

In practice, it is common to approximate the friction cone $\mathcal{F}_{c_i}(\mu)$ by an inscribed pyramid with $l_s \in \mathbb{N}$ sides [19], [24]. The set associated with this inscribed pyramid is defined as

$$\mathring{\mathcal{F}}_{c_i}(\mu) \coloneqq \{\boldsymbol{f}_{c_i}^{\mathcal{C}_i} \in \mathbb{R}^3 : \Lambda_i(\mu)\boldsymbol{f}_{c_i}^{\mathcal{C}_i} \succeq \mathbf{0}\} \tag{9}$$

where $\Lambda_i : \mathbb{R}_{>0} \to \mathbb{R}^{l_s \times 3}$ is a matrix defining the pyramid. Similarly, the friction pyramid is defined as the Cartesian product of all $\mathring{\mathcal{F}}_{c_i}$, which is equivalent to concatenating all $\Lambda_i(\mu)$ into $\Lambda(\mu) = \text{diag}\{\Lambda_1, ..., \Lambda_N\}$. The resulting set is then $\mathring{\mathcal{F}}_c \coloneqq \{\boldsymbol{f}_c^{\mathcal{C}} \in \mathbb{R}^{3N} : \Lambda(\mu)\boldsymbol{f}_c^{\mathcal{C}} \succeq \mathbf{0}\}$. Note that if $\boldsymbol{f}_{c_i} \in \mathring{\mathcal{F}}_{c_i}$, then the contact force always has a positive normal component (i.e. the manipulators cannot "pull" on the contact point). Substitution of $\boldsymbol{f}_{c_i}^{\mathcal{C}_i} = R_{pc_i}^\top \boldsymbol{f}_{c_i}$, and concatenation over all $i \in \mathcal{N}$ yields:

$$\Lambda(\mu)R_{pc}^\top \boldsymbol{f}_c \succeq 0, \tag{10}$$

where $R_{pc} \coloneqq \text{diag}\{[R_{pc_i}]_{i\in\mathcal{N}}\}$, $\Lambda(\mu) \coloneqq \text{diag}\{[\Lambda_i(\mu)]_{i\in\mathcal{N}}\}$.

The following standard assumption is made for the grasp to ensure the existence of contact forces for slip prevention:

Assumption 1. *The grasp consists of $N \geq 3$ agents with non-collinear contact points and $\mathfrak{N}(G) \bigcap \text{Int}(\mathring{\mathcal{F}}_c) \neq \emptyset$.*

Note that $N \geq 3$ agents with non-collinear contact points ensures G is full row rank [21]. The condition that $\mathfrak{N}(G) \bigcap \text{Int}(\mathring{\mathcal{F}}_c) \neq \emptyset$ ensures the existence of a contact force that lies within the friction cone and yields a desired object wrench, which is called the force-closure condition [8]. Force-closure depends on the initial grasp, and can be ensured by existing high-level grasp planning methods [25].

Slip prevention is addressed by ensuring that the no-slip condition (10) holds. In particular, we guarantee that (10) holds by designing an internal force controller $\boldsymbol{f}_{\text{int}_k} \in \mathbb{R}^{3N}$ as follows:

$$\boldsymbol{f}_{\text{int}_k} = R_{pc_k}\boldsymbol{\ell}_k^* \tag{11a}$$

$$\boldsymbol{\ell}_k^* = \text{argmin}_{\boldsymbol{\ell}\in\mathbb{R}^{3N}} \ \boldsymbol{\ell}^\top\boldsymbol{\ell} \tag{11b}$$

$$\text{s. t.} \tag{11c}$$

$$G_k R_{pc_k}\boldsymbol{\ell} = 0_6 \tag{11d}$$

$$\Lambda(\mu)\boldsymbol{\ell} \succeq \varepsilon \mathbf{1}_{3N}, \tag{11e}$$

where $\varepsilon \in \mathbb{R}_{>0}$ is a design parameter. Here (11d) ensures the internal force remains in the null space of G_k to not interfere with the reference tracking task and (11e) ensures the internal force is sufficiently inside the friction cone to prevent slip. The term ε is used to account for dynamics and uncertainties in G_k, R_{pc_k} that may cause slip. Note that $\boldsymbol{f}_{\text{int}_k}$ is constant for $t \in [t_k, t_{k+1})$ such that it needs only be computed at each k update. We note that $\boldsymbol{f}_{\text{int}_k}$ is the concatenation of all agents' internal forces $\boldsymbol{f}_{\text{int}_{k,i}} \in \mathbb{R}^3$. Thus, at each event, agent i computes (11) and implements the respective component $\boldsymbol{f}_{\text{int}_{k,i}}$.

To ensure slip prevention for the proposed control, we need an additional assumption:

Assumption 2. *There exists a $\bar{l} \in \mathbb{R}_{>0}$ such that, for any $k \in \mathbb{N}$, there exists a $\|\boldsymbol{\ell}\|_2 \leq \bar{l}$ satisfying* (11d) *and* (11e)*.*

Assumption 2 is a practical assumption stating that there exists a bounded contact force to satisfy the no-slip condition. We introduce the following lemma to ensure no slip between events.

Lemma 1. *Let a matrix $W \in \mathbb{R}^{3N\times 3N}$ and a vector $\boldsymbol{l}_k \in \mathbb{R}^{3N}$ satisfying $\|W\|_\infty \leq \delta_c$ and $\|\boldsymbol{l}_k\|_\infty \leq \bar{l}$, for some positive constants $\delta_c, \bar{l}$. Further assume that $\|\Lambda(\mu)\|_\infty \leq \lambda$ for a positive constant λ. If, for a given $\varepsilon_h \in \mathbb{R}_{>0}$, $\Lambda(\mu)\boldsymbol{l}_k \succeq (\varepsilon_h + \lambda\delta_c\bar{l})\mathbf{1}_{3N}$, then $\Lambda(\mu)(I_{3N\times 3N} - W)\boldsymbol{l}_k \succeq \varepsilon_h \mathbf{1}_{3N}$.*

Proof. Let $\boldsymbol{z} = -\Lambda(\mu)W\boldsymbol{l}_k$ be a perturbation on the term $\Lambda(\mu)\boldsymbol{l}_k$, with bound $\|\boldsymbol{z}\|_\infty \leq \|-\Lambda(\mu)W\boldsymbol{l}_k\|_\infty \leq \lambda\delta_c\bar{l}$. It follows then that $\boldsymbol{z} \succeq -\lambda\delta_c\bar{l}\mathbf{1}_{3N}$. Thus, $\Lambda(\mu)(I_{3N\times 3N} - W)\boldsymbol{l}_k = \Lambda(\mu)\boldsymbol{l}_k - \Lambda(\mu)W\boldsymbol{l}_k \succeq (\varepsilon_h + \lambda\delta_c\bar{l} - \lambda\delta_c\bar{l})\mathbf{1}_{3N} \succeq \varepsilon_h\mathbf{1}_{3N}$. □

In Lemma 1, the matrix W represents the error associated with $G - G_k$ and $R_{pc}^\top R_{pc_k} - I_{3N\times 3N}$ due to the lack of communication between agents between events. The constant ε_h is a robustness term that bounds the system dynamics to prevent slip. The additional robustness margin $\lambda\delta_c\bar{l}$ is required to ensure the perturbations from G_k and R_{pc_k} do not push the contact force outside the friction cone and thus cause slip.

C. Adaptive Updates and Distributed Control Law

When the contact points do not slip, the grasp relation $J_h\dot{\boldsymbol{q}} = \bar{G}^\top\bar{\boldsymbol{v}}_o$ holds [8], which, after substituting (8), becomes:

$$\boldsymbol{v}_c = J_h\dot{\boldsymbol{q}} = G^\top\boldsymbol{v}_o, \tag{12}$$

where $\boldsymbol{v}_c \coloneqq [\boldsymbol{v}_{c_1}^\top, \ldots, \boldsymbol{v}_{c_N}^\top]^\top \in \mathbb{R}^{3N}$ is the vector of contact velocities. We make the following standard assumption:

Assumption 3. *The matrix $J_h(\boldsymbol{q})$ is non-singular, and the contact points do not exceed the end-effector surface throughout the manipulation task.*

Remark 1. *By incorporating optimization techniques, as e.g. in [26], we can enforce prevention of excessive rolling of the contacts and thus relax the respective part of Assumption 3. The non-singular condition of J_h intuitively implies that tracking the desired reference trajectory does not force the agents through such singular configurations. This can also be achieved by exploiting internal motions of redundant agents ($n_i > 3$). If contact loss is prevented, the full row rank condition of G implies the existence of a $\underline{g} > 0$ such that $\lambda_{\min}(GG^\top) \geq \underline{g}$.*

Moreover, the following Lemma will be needed in the subsequent analysis.

Lemma 2. *[5] The matrices $M_i(\boldsymbol{q}_i)$, $\bar{M}_o(\bar{\boldsymbol{\eta}}_o)$ are symmetric and positive-definite, and $\dot{M}_i(\boldsymbol{q}_i) - 2C_i(\boldsymbol{q}_i, \dot{\boldsymbol{q}}_i)$, $\dot{\bar{M}}_o(\bar{\boldsymbol{\eta}}_o) - 2\bar{C}_o(\bar{\boldsymbol{\eta}}_o, \bar{\boldsymbol{\omega}}_o)$ are skew-symmetric, for all $\boldsymbol{q}_i, \dot{\boldsymbol{q}}_i \in \mathbb{R}^{n_i}, i \in \mathcal{N}, \bar{\boldsymbol{\eta}}_o, \bar{\boldsymbol{\omega}}_o \in \mathbb{M}\times\mathbb{R}^6$.*

In view of Lemma 2, one can verify that M_o is positive definite and $\dot{M}_o - 2C_o$ is skew-symmetric as well. We also assume that the contact vectors $\boldsymbol{p}_{fc_i}^{\mathcal{F}_i}$ and $\dot{\boldsymbol{p}}_{fc_i}^{\mathcal{F}_i}$ are measured accurately online, for all $i \in \mathcal{N}$. This can be achieved by the use of tactile sensors that provide contact location.

Without loss of generality, we assume that $n_i = 3$, $\forall i \in \mathcal{N}$, i.e., the agents are not redundant. The proposed solution can be extended to redundant cases, e.g., by following the analysis of [21, Chapter 6]. By combining the agent and object dynamics (2), (7) as well as (12), we obtain the coupled dynamics:

$$\tilde{M}\dot{\boldsymbol{v}}_o + \tilde{C}\boldsymbol{v}_o + \tilde{\boldsymbol{g}} = GJ_h^{-T}\boldsymbol{u}, \tag{13}$$

where $\tilde{M} := \tilde{M}(\tilde{\boldsymbol{x}}) := M_o + GJ_h^{-T}MJ_h^{-1}G^\top$, $\tilde{C} := \tilde{C}(\tilde{\boldsymbol{x}}, \dot{\tilde{\boldsymbol{x}}}) := C_o + GJ_h^{-T}(CJ_h^{-1}G^\top + M\frac{d}{dt}(J_h^{-1}G^\top))$, $\tilde{\boldsymbol{g}} := \tilde{\boldsymbol{g}}(\tilde{\boldsymbol{x}}) := \boldsymbol{g}_o + GJ_h^{-T}\boldsymbol{g}$, and $\tilde{\boldsymbol{x}} := [\boldsymbol{\eta}_o^\top, \boldsymbol{q}^\top, \boldsymbol{p}_{fc}^\top, \boldsymbol{p}_{oc}^\top]^\top \in \mathsf{S}^3 \times \mathbb{R}^{n+6N}$. The following lemma, which can be derived using Lemma 2, states useful properties of (13):

Lemma 3. *[5] The matrix $\tilde{M}$, is symmetric and positive-definite, and $\dot{\tilde{M}} - 2\tilde{C}$ is skew-symmetric.*

The left-hand side of the object dynamics can be linearly parameterized with respect to the dynamic parameters as:

$$M_o(\boldsymbol{\eta}_o)\dot{\boldsymbol{v}}_o + C_o(\boldsymbol{\eta}_o, \boldsymbol{\omega}_o)\boldsymbol{v}_o + \boldsymbol{g}_o = Y_o(\boldsymbol{\eta}_o, \boldsymbol{\omega}_o, \boldsymbol{v}_o, \dot{\boldsymbol{v}}_o)\boldsymbol{\nu}_o,$$

where $\boldsymbol{\nu}_o \in \mathbb{R}^{l_o}$, $l_o \in \mathbb{N}$, is a vector containing unknown object dynamic parameters as well as the term $\boldsymbol{p}_{\mathcal{O}o}^{\mathcal{O}}$, introduced in (6), and $Y_o : \mathsf{S}^3 \times \mathbb{R}^{18} \to \mathbb{R}^{6\times l_o}$ is a known regressor matrix.

Similarly, the dynamic parameters of the agents from (13) can be linearly parameterized [20]:

$$MJ_h^{-1}G^\top\dot{\boldsymbol{v}}_o + \left(M\frac{d}{dt}(J_h^{-1}G^\top) + CJ_h^{-1}G^\top\right)\boldsymbol{v}_o + \boldsymbol{g} = Y(\tilde{\boldsymbol{x}}, \dot{\tilde{\boldsymbol{x}}}, \boldsymbol{v}_o, \dot{\boldsymbol{v}}_o)\boldsymbol{\nu},$$

where $\boldsymbol{\nu} \in \mathbb{R}^l, l \in \mathbb{N}$, is a vector of unknown dynamic parameters of the agents, and $Y : \mathsf{S}^3 \times \mathbb{R}^{2n+15N} \to \mathbb{R}^{6N\times l}$ is the respective known regressor matrix. Note this regressor can be formulated in a distributed manner by exploiting the block diagonal structure of M and J_h:

$$M_iJ_{h_i}^{-1}G_i^\top\dot{\boldsymbol{v}}_o + \left(M_i\frac{\partial}{\partial t}(J_{h_i}^{-1}G_i^\top) + C_iJ_{h_i}^{-1}G_i^\top\right)\boldsymbol{v}_o + \boldsymbol{g}_i = Y_i(\tilde{\boldsymbol{x}}_i, \dot{\tilde{\boldsymbol{x}}}_i, \boldsymbol{v}_o, \dot{\boldsymbol{v}}_o)\boldsymbol{\nu}_i,$$

where $\tilde{\boldsymbol{x}}_i = [\boldsymbol{\eta}_o^\top, \boldsymbol{q}_i^\top, \boldsymbol{p}_{fc_i}^\top, \boldsymbol{p}_{oc}^\top]^\top$, $Y = \text{diag}\{[Y_i]_{i\in\mathcal{N}}\}$, and $\boldsymbol{\nu} = [\boldsymbol{\nu}_1^\top, ..., \boldsymbol{\nu}_N^\top]^\top$. The linear parameterization of the dynamics is achieved by separating the dynamic parameters from the functions defined in the regressor matrix. In practice, this can be done using symbolic methods in Python/Matlab.

The left-hand side of (13) can be written as:

$$\tilde{M}\dot{\boldsymbol{v}}_o + \tilde{C}\boldsymbol{v}_o + \tilde{\boldsymbol{g}} = Y_o(\boldsymbol{\eta}_o, \boldsymbol{\omega}_o, \boldsymbol{v}_o, \dot{\boldsymbol{v}}_o)\boldsymbol{\nu}_o + GJ_h^{-T}Y(\tilde{\boldsymbol{x}}, \dot{\tilde{\boldsymbol{x}}}, \boldsymbol{v}_o, \dot{\boldsymbol{v}}_o)\boldsymbol{\nu} \tag{14}$$

Let now $\hat{\boldsymbol{\nu}} \in \mathbb{R}^l$, $\hat{\boldsymbol{\nu}}_o \in \mathbb{R}^{l_o}$, be estimates of $\boldsymbol{\nu}$ and $\boldsymbol{\nu}_o$, respectively, by the agents, and the respective errors $\boldsymbol{e}_\nu := \hat{\boldsymbol{\nu}} - \boldsymbol{\nu}$, and $\boldsymbol{e}_{\nu_o} := \hat{\boldsymbol{\nu}}_o - \boldsymbol{\nu}_o$.

As described in Problem 1, the pose errors are $\boldsymbol{e}_p = \boldsymbol{p}_o - \boldsymbol{p}_\text{d}$ and $\boldsymbol{e}_\eta = \boldsymbol{\eta}_\text{d} \otimes \boldsymbol{\eta}_o^+$, which can be shown to satisfy [5]:

$$\boldsymbol{e}_\eta = \begin{bmatrix} e_\varphi \\ \boldsymbol{e}_\epsilon \end{bmatrix} := \begin{bmatrix} \varphi_o\varphi_\text{d} + \boldsymbol{\epsilon}_o^\top\boldsymbol{\epsilon}_\text{d} \\ \varphi_o\boldsymbol{\epsilon}_\text{d} - \varphi_\text{d}\boldsymbol{\epsilon}_o + (\boldsymbol{\epsilon}_o)\times\ \boldsymbol{\epsilon}_\text{d} \end{bmatrix}. \tag{15a}$$

$$\dot{\boldsymbol{e}}_p = \dot{\boldsymbol{p}}_o - \dot{\boldsymbol{p}}_\text{d} \tag{15b}$$

$$\dot{\boldsymbol{e}}_\eta = \begin{bmatrix} \dot{e}_\varphi \\ \dot{\boldsymbol{e}}_\epsilon \end{bmatrix} = \begin{bmatrix} \frac{1}{2}\boldsymbol{e}_\epsilon^\top\boldsymbol{e}_\omega \\ -\frac{1}{2}(e_\varphi I_3 + (\boldsymbol{e}_\epsilon)\times)\boldsymbol{e}_\omega - (\boldsymbol{e}_\epsilon)\times\ \dot{\boldsymbol{\omega}}_\text{d} \end{bmatrix}, \tag{15c}$$

where $\boldsymbol{e}_\omega := \boldsymbol{\omega}_o - \boldsymbol{\omega}_\text{d} \in \mathbb{R}^3$ and $\boldsymbol{\omega}_\text{d} = 2E(\boldsymbol{\eta}_\text{d})\dot{\boldsymbol{\eta}}_\text{d}$, similarly to (4).

The reference velocity signal $\boldsymbol{v}_f \in \mathbb{R}^6$ and the associated velocity error $\boldsymbol{e}_v$ are defined by

$$\boldsymbol{v}_f := \boldsymbol{v}_\text{d} - K\boldsymbol{e} := \begin{bmatrix} \dot{\boldsymbol{p}}_\text{d} \\ \boldsymbol{\omega}_\text{d} \end{bmatrix} - \begin{bmatrix} k_p\boldsymbol{e}_p \\ -k_\eta\frac{\boldsymbol{e}_\epsilon}{e_\varphi^3} \end{bmatrix} \tag{16a}$$

$$\boldsymbol{e}_v := \boldsymbol{v}_o - \boldsymbol{v}_f, \tag{16b}$$

where $K := \text{diag}\{k_pI_3, k_\eta I_3\} \in \mathbb{R}^3$ is a positive definite gain matrix, with k_p, k_η positive constants, $\boldsymbol{e} := [\boldsymbol{e}_p^\top, -\frac{\boldsymbol{e}_\epsilon^\top}{e_\varphi^3}]^\top$, and $\boldsymbol{v}_\text{d} := [\dot{\boldsymbol{p}}_\text{d}^\top, \boldsymbol{\omega}_\text{d}^\top]^\top$. As will be shown later, $e_\varphi(0) \neq 0 \Rightarrow e_\varphi(t) \neq 0$, $\forall t \geq 0$, thus (16a) is well defined.

Next, we present the distributed control algorithm that uses event-triggered communication among the agents to track the desired reference trajectory:

$$\boldsymbol{u}_{k_i} = Y_{r_i}\hat{\boldsymbol{\nu}}_i + J_{h_i}^\top(\boldsymbol{\lambda}_{k_i} + \boldsymbol{f}_{\text{int}_{k,i}}), \tag{17a}$$

$$\boldsymbol{\lambda}_{k_i} := -G_i^\top K_v\boldsymbol{e}_v + G_{k_i}^*(Y_{o_r}\hat{\boldsymbol{\nu}}_o - \boldsymbol{e}) \tag{17b}$$

where $Y_{r_i} := Y(\tilde{\boldsymbol{x}}_i, \dot{\tilde{\boldsymbol{x}}}_i, \boldsymbol{v}_f, \dot{\boldsymbol{v}}_f)$, $Y_{o_r} := Y_o(\boldsymbol{\eta}_o, \boldsymbol{\omega}_o, \boldsymbol{v}_f, \dot{\boldsymbol{v}}_f)$, $K_v \in \mathbb{R}^{6\times6}$ is positive-definite and diagonal, and $G_k^* = [G_{k_1}^{*^\top}, ..., G_{k_N}^{*^\top}]^\top$ is the generalized inverse of the grasp map at $t = t_k$. We design the adaptation signals as

$$\dot{\hat{\boldsymbol{\nu}}}_i = \text{Proj}(\hat{\boldsymbol{\nu}}_i, -\Gamma Y_{r_i}^\top J_{h_i}^{-1}G_i^\top\boldsymbol{e}_v), \tag{18a}$$

$$\dot{\hat{\boldsymbol{\nu}}}_o = \text{Proj}(\hat{\boldsymbol{\nu}}_o, -\Gamma_o Y_{o_r}^\top\boldsymbol{e}_v), \tag{18b}$$

where $\Gamma \in \mathbb{R}^{l\times l}, \Gamma_o \in \mathbb{R}^{l_o\times l_o}$ are positive-definite constant matrices, and Proj() is the projection operator satisfying: [27]:

$$(\hat{\boldsymbol{\theta}} - \boldsymbol{\theta})^\top(A^{-1}\text{Proj}(\hat{\boldsymbol{\theta}}, A\boldsymbol{z}) - \boldsymbol{z}) \leq \boldsymbol{0}_{l_z}, \tag{19}$$

for any symmetric positive definite $A \in \mathbb{R}^{l_z\times l_z}$, and $\forall\boldsymbol{\theta}, \hat{\boldsymbol{\theta}}, \boldsymbol{z} \in \mathbb{R}^{l_z}$, for some $l_z \in \mathbb{N}$. Moreover, by appropriately choosing the initial conditions of the estimates $\hat{\boldsymbol{\nu}}(0)$, $\hat{\boldsymbol{\nu}}(0)$, the projection operator ensures that $\hat{\boldsymbol{\nu}}(t)$, $\hat{\boldsymbol{\nu}}(t)$ will stay uniformly bounded in predefined sets defined by finite constants $\bar{\boldsymbol{\nu}}$, $\bar{\boldsymbol{\nu}}_o$, i.e., $\|\hat{\boldsymbol{\nu}}(t)\| \leq \bar{\boldsymbol{\nu}}$, $\|\hat{\boldsymbol{\nu}}_o(t)\| \leq \bar{\boldsymbol{\nu}}_o$, $\forall t \geq 0$ [27]. Hence, we can achieve the boundedness of the respective errors as

$$\|\boldsymbol{e}_\nu(t)\| \leq \bar{e}_\nu := \bar{\boldsymbol{\nu}} + \|\boldsymbol{\nu}\| \tag{20a}$$

$$\|\boldsymbol{e}_{\nu_o}(t)\| \leq \bar{e}_{\nu_o} := \bar{\boldsymbol{\nu}}_o + \|\boldsymbol{\nu}_o\|, \tag{20b}$$

for finite constants $\bar{e}_\nu, \bar{e}_{\nu_o}$ (see [27, Chapter 11] for more details). Note that the adaptation signals (18) are only dependent on local information $\boldsymbol{q}_i$, $\boldsymbol{p}_{fc_i}$ and the broadcast signals $\boldsymbol{x}_o$, $\dot{\boldsymbol{x}}_o$.

D. Event-triggering Updates

Now that the slip prevention and trajectory tracking controllers are defined, we can present the event-triggering conditions. First, we note that the only elements of (11) and (17) that depend on inter-agent communication are R_{pc_k}, G_k, and $G_{k_i}^*$. Further note that each agent has knowledge of its own G_i since it is only dependent on local measurements. However, the inverse G_k^* is dependent on knowledge of all $\boldsymbol{p}_{oc_i}$ and so is only updated at events. The broadcast signals $\boldsymbol{p}_{oc_{k,i}}$, $\boldsymbol{\eta}_{pc_{k,i}}$ jeopardize the control law because they are not continuously communicated between all agents. To address the lack of communication, we introduce the event-triggering conditions to define when these terms need to be updated:

$$||\Delta \boldsymbol{p}_{oc_i}|| = \delta_p \tag{21}$$

$$||R_{pc_i}^\top R_{pc_{k,i}} - I_{3\times 3}|| = \delta_r \tag{22}$$

$$\boldsymbol{e}_v^\top \begin{bmatrix} 0_{3\times 3} \\ (\Delta \boldsymbol{p}_{oc_i})\times \end{bmatrix} \left(\boldsymbol{f}_{\text{int}_{k,i}} + G_{k_i}^* Y_{or} \hat{\boldsymbol{\nu}}_o \right) - c_2 \gamma = 0 \tag{23}$$

with $\Delta \boldsymbol{p}_{oc_i} = \boldsymbol{p}_{oc_i} - \boldsymbol{p}_{oc_{k,i}}$, $k_1 \coloneqq \lambda_{\min}(K)$, $k_2 \coloneqq \min_{\boldsymbol{p}_{oc}} \lambda_{\min}(G(\boldsymbol{p}_{oc})G(\boldsymbol{p}_{oc})^\top K_v)$, and γ, $c_2 \in (0, \min\{k_1, k_2\})$ are design parameters. The bound δ_p is constant between events and is defined by

$$\delta_p := \min \left\{ \frac{2}{\sum_i ||G_{k_i}^*||} \min\{k_1 - c_2, k_2 - c_2\}, \frac{\delta_c}{2\varepsilon_c} \right\}$$

for design parameters $\varepsilon_c, \delta_c \in \mathbb{R}_{>0}$. Note that by construction δ_p is always positive and bounded. Furthermore, the full rank condition on G ensures that $G_{k_i}^*$ exists and $\|G_{k_i}^*\| \neq 0$. The term δ_r is a constant satisfying $\delta_r < \frac{\delta_c}{2\varepsilon_c}$. Finally, note that $k_2 > 0$ due to the fact that G is full row rank (see Remark 1).

We note that many design parameters are introduced in (21), (22), and (23), which will be explained as follows. The first term in δ_p is required to ensure stability of the closed-loop system. The second term of δ_p ensures that the errors that arise from G_k, i.e., $G - G_k$, are sufficiently small to prevent slip. The condition for δ_r is similarly defined to ensure errors from R_{pc_k}, i.e. $R_{pc}^\top R_{pc_k} - I_{3N\times 3N}$, are small. Finally, condition (23) is required to ensure ultimate-boundedness of the closed loop system wherein the ultimate bound is determined by γ. This condition is necessary due to the product of the erroneous $G_{k_i}^*$ in the control (17). We note that a smaller ultimate bound (i.e. smaller γ) may require more communication between agents as seen in (23). In effect, γ acts as a tuning parameter that defines a trade-off between communication and performance, i.e., more communication yields better tracking and vice versa. Also, the approach avoids Zeno behaviour (this is formally shown in the proof of Theorem (1)). Intuitively, the right-hand sides of (21) and (22) are strictly positive, and thus the left-hand sides become 0 at triggering times. Moreover, as shown in the proof of Theorem (1), the continuity and boundedness (in compact sets) of the terms in the left-hand sides renders the inter-event times positive and lower-bounded (similar arguments hold for (23)).

The time instants when an event is triggered is when (21), (22), or (23) are satisfied, and formally defined as:

$$t(0) = 0,\ t_{k+1} = \inf\{t \in \mathbb{R} : t > t_k \wedge ((21) \vee (22) \vee (23))\} \tag{24}$$

The event is triggered when the contact points roll excessively far such that $\boldsymbol{p}_{oc_{k,i}}$, $R_{pc_{k,i}}$ exceed the pre-defined errors or the tracking error is too large. The condition (24) is evaluated by each agent individually. When one agent identifies a triggering condition, the agent then signals to all agents that an update is required and all agents then broadcast *only* their local $\boldsymbol{p}_{oc_i}$ and $\boldsymbol{\eta}_{pc_i}$ for all $i \in \mathcal{N}$, which allows them to compute G_k, R_{pc_k}, $G_{k_i}^*$, and $\boldsymbol{f}_{\text{int}_{k,i}}$ to implement the proposed control.

Theorem 1. *Consider N robotic agents in contact with an object, described by the dynamics* (2)*,* (7)*, and suppose Assumptions 1-3 hold. Let the desired object pose* ($\boldsymbol{p}_\text{d}$, $\boldsymbol{\eta}_\text{d}$) $: \mathbb{R}_{\geq 0} \to \mathbb{R}^3 \times \mathsf{S}^3$ *be bounded with bounded first and second derivatives and consider the stack vector state* $\boldsymbol{\chi} \coloneqq [\boldsymbol{e}_p^\top, \frac{\boldsymbol{e}_\epsilon}{e_\phi}^\top, \boldsymbol{e}_v^\top, \boldsymbol{e}_\nu^\top, \boldsymbol{e}_{\nu_o}^\top]^\top \in \mathcal{X} \coloneqq \mathbb{R}^{12+\ell+\ell_o}$*. Moreover, assume that $e_\varphi(0) \neq 0$ and $\boldsymbol{f}_{c_i}^{C_i}(0) \in Int(\mathring{\mathcal{F}}_{c_i})$, $\forall i \in \mathcal{N}$. Then, for sufficiently large control gains ε, ε_c, the event-triggered control protocol* (17)*,* (18)*,* (11) *with event-triggered mechanism* (24) *guarantees (a) avoidance of Zeno behavior, (b) $\boldsymbol{f}_c^{C_i}(t) \in \mathcal{F}_{c_i}, \forall t > 0$, $i \in \mathcal{N}$, and (c) the existence of class-$\mathcal{K}$ functions α_1, α_2, a class-$\mathcal{KL}$ function β, and $T_1, T_2, \rho_\gamma, \bar{\delta}, k_\chi \in \mathbb{R}_{>0}$ such that the following hold:*

$$\|\boldsymbol{e}\|^2 + \|\boldsymbol{e}_v(t)\|^2 \leq \rho_\gamma, \forall t \geq T_1, \tag{25}$$

$$\|\boldsymbol{\chi}(t)\| \leq \beta(\|\boldsymbol{\chi}(0)\|, t),\ \forall t \in [0, T_2), \tag{26}$$

$$\|\boldsymbol{\chi}(t)\| \leq \alpha_1^{-1}(\alpha_2(\sqrt{\frac{\bar{\delta}}{k_\chi}})), \forall t \geq T_2. \tag{27}$$

Proof. See Appendix. □

Remark 2. *Note that the lower bounds for ε and ε_c as needed in the proof of Theorem 1 (see Appendix) can be computed a priori. In practice, the terms ν, ν_o, which concern masses and moments of inertia of the object and the agents, can be known a priori up to a certain accuracy, leading thus to respective bounds. Hence, one can compute upper bounds for $V(0)$ (see proof of Theorem 1) and hence for $\boldsymbol{e}$, $\boldsymbol{e}_v$, $\boldsymbol{e}_\nu$, and $\boldsymbol{e}_{\nu_o}$. Also, since the structure of the dynamic terms is known, their approximate bounds can be computed, which allows for off-line computation of ε and ε_c.*

Remark 3 (Effect of $\gamma, \delta_p, \delta_r$)**.** *The parameter γ yields a monotonically increasing relationship with ρ_γ, which provides a trade-off between communication frequency and ultimate bound as per* (25)-(27) *and* (30)*. In other words, as γ decreases, the ultimate bound decreases. The term δ_p dictates the maximum allowable error in ΔG, which directly affects the ultimate bound in* (30)*. The terms δ_r and δ_p affect the magnitude of $\boldsymbol{f}_{int_k}$ and thus the ultimate bound from* (30)*, as follows. As δ_r and δ_p decrease, the magnitude of W in* (33) *decreases, yielding smaller disturbance due to communication lag and thus requires a smaller ε. A smaller ε yields a smaller*

magnitude $\boldsymbol{f}_{int_k}$ as per (11)*, which results in smaller ultimate bound due to* (30)*.*

E. Implementation

We have presented a novel, event-triggered control law to reduce the communication needed for cooperative mobile manipulators to manipulate objects. Our formulation assumes force/torque control of all robot agents. In practice, it is common for the mobile bases to be controlled via position/velocity commands, which does not fit within our framework.

To account for non-force/torque commanded mobile-bases, one can use standard formation controllers [28] to keep the mobile bases in a desired formation throughout the entire manipulation trajectory. This has the advantage of reducing complexity when, for example, avoiding obstacles, since the mobile bases can be controlled in formation, independent of the manipulators. In such a case, we exploit the redundancy in the mobile manipulator to let the bases navigate the 2-dimensional plane, while the manipulators manipulate outside of the plane. Then, the 'inertial frame' $\mathscr{P}$ is fixed to the mobile base formation, which each agent can determine independently once the formation is formed at the start of the manipulation task. In practice, the motion of the inertial frame will be seen as a disturbance on the inertial-frame related terms. However, the ultimate boundedness guarantees from Theorem 1 ensure that for sufficiently slow formation movements, these disturbances will not de-stabilize the system.

The proposed method can handle objects of various shapes due to the internal force controller (11). If knowledge of the object shape is known a priori, then the quadratic program from (11) can be replaced by a closed-form solution, which avoids solving an optimization problem online. Consider, for example, spherical objects, which can be difficult or even impossible for a gripper to form a rigid grasp on. If the initial formation of the agents is distributed evenly around the sphere (i.e., the agents form a so-called optimal grasp [29]), then we can also exploit the symmetry of the formation to avoid the computation of (11), as shown in the following lemma.

Lemma 4. *Consider a spherical object with radius $r \in \mathbb{R}_{>0}$, wherein the contact points of all agents are equi-distantly distributed on the surface of the object and lie in the equatorial plane. Let the internal force control be $\boldsymbol{f}_{int_{k_i}} = \frac{\varepsilon}{r\mu}\boldsymbol{z}_i$, with $\boldsymbol{z}_i = \frac{1}{N}(\sum_{i\in\mathcal{N}} \boldsymbol{p}_{oc_i}) - \boldsymbol{p}_{oc_i}$ for $i \in \mathcal{N}$ and $\boldsymbol{p}_o$ designates the geometric center of the object. Then, the internal force controller solves* (11) *with $\|\boldsymbol{\ell}\|_2 = \bar{l} = \sqrt{N}\frac{\varepsilon}{\mu}$.*

Proof. It is clear that the contact normal for each ith agent is $\frac{\boldsymbol{z}_i}{\|\boldsymbol{z}_i\|}$. Also, due to the symmetry of the contact points, $\boldsymbol{p}_o = \frac{1}{N}\sum_{i\in\mathcal{N}} \boldsymbol{p}_{oc_i}$ and $\|\boldsymbol{z}_i\| = r$. Now it is clear that $G_k \boldsymbol{f}_{\text{int}_k} = 0$ by definition of G_k with $\boldsymbol{p}_o$ located at the spherical object's center. Next, we can write the internal force control in the contact frame of each agent as: $\boldsymbol{\ell}_{k_i} = R^T_{pc_{k_i}} \boldsymbol{f}_{\text{int}_{k_i}} = \frac{\varepsilon}{r\mu}[0, r, 0]^T = \frac{\varepsilon}{\mu}[0, 1, 0]^T$, where without loss of generality we assume the second axis of the contact frame is aligned with the normal direction and has magnitude $f_{n_i} = \frac{\varepsilon}{\mu}$. Since the internal force only acts in the normal direction, from (5), we see that $f_{n_i}\mu = \varepsilon \geq 0 = \sqrt{f_{x_i}^2 + f_{y_i}^2}$. Thus $\boldsymbol{\ell}_{k_i}$ is in the friction cone and has a lower bound on the normal force: $f_{n_i} = \frac{\varepsilon}{\mu}$. It can now be deduced that this implies $\Lambda(\mu)\boldsymbol{\ell}_k \succeq \varepsilon \mathbf{1}_{3N}$. Finally, we can compute $\|\boldsymbol{\ell}_k\|_2 = \sqrt{\sum_{i\in\mathcal{N}}(\frac{\varepsilon}{\mu})^2} = \sqrt{N}\frac{\varepsilon}{\mu}$. □

Lemma 4 provides a closed-form solution for which the bound of the internal force control is easily computed a priori. However, the results of Lemma 4 only hold when the contact points are equi-distant on the object surface. In practice, the contact points may deviate from these positions as they roll during the manipulation task. As a result, we have found that larger values of ε are required to account for such deviations in practice, as will be shown in the next section.

IV. Hardware Results

In this section, we implement the proposed controller to manipulate several objects. We also demonstrate how the proposed control can be used to track an object reference that transports an object through an environment. We used the mobile manipulators HEBI A-2160-01, named "Rosie", which have an omni-directional base with a 3DOF robotic arm. We removed the gripper from the HEBI arm and replaced it with a 3D printed hemispherical passive end-effector, shown in Figure 1. We emulated tactile sensing by using the object shapes and location of the object and agent end-effectors using the method discussed in [30]. The proposed control was implemented using ROS Kinetic in Python.

To showcase the results, we consider three objects of varying mass/inertia, shape, and size. These objects include a hexagonal prism (denoted 'hex'), a soccer ball (denoted 'ball'), and a cubic box (denoted 'box'), which are shown in Figure 2. The respective masses of the hex, ball, and box are $71g$, $350g$, and $450g$. Here we focus on the application of our controller to different object sizes and shapes, and so keep the friction coefficient μ constant, estimated to be $\mu = 1.2$, by applying tape (blue strips in Figure 2) on the objects' surfaces.

For each agent, a ROS node was launched to compute the respective control law. Each node has a loop, which contains the calculations of (21)-(23). During this loop, if the event condition was satisfied by agent j, then agent j would publish to a node that all agents are subscribed to to indicate that an event has occurred. Once this happens, all agents publish their measurements of $\boldsymbol{p}_{oc_{i,k}}$ and $\boldsymbol{\eta}_{pc_{i,k}}$ to all other agents. Each agent then updates their stored values of $\boldsymbol{p}_{oc_k}$ and $\boldsymbol{\eta}_{pc_k}$.

The proposed controller is implemented with a practical perspective by taking into consideration the fact that, prior to any manipulation task, an initial grasp must be formed. This can be done using existing grasp planning algorithms in which the size/shape of the object is approximately known a priori. Also, an initial 'good' estimate of the object mass/inertia can be provided. The important distinction in our implementation is that we do not assume these properties exactly known. The adaptive component in our controller allows for each agent to estimate the model parameters, which vary inside their parameter sets. In this demonstration, the parameter sets are the same for all objects and set as $[0.05, .85]$. Furthermore,

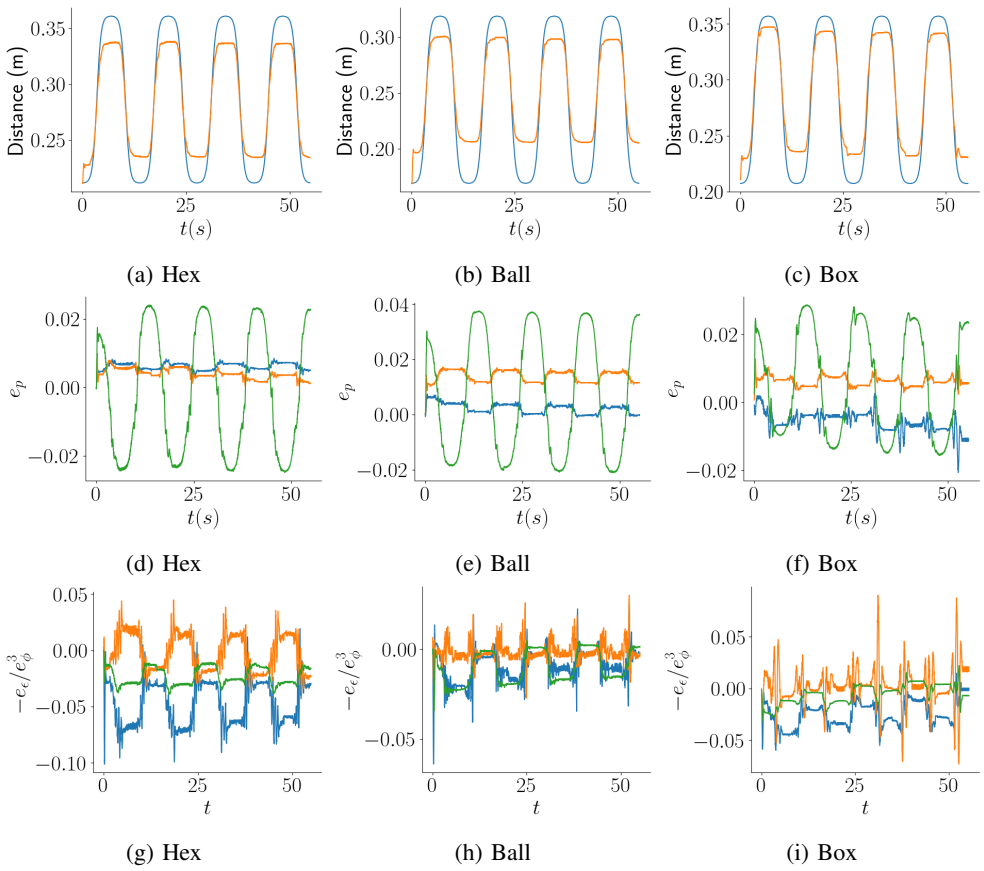

(a) Hex (b) Ball (c) Box

(d) Hex (e) Ball (f) Box

(g) Hex (h) Ball (i) Box

Fig. 4: Comparison of trajectories for tracking Z-translation amongst the hex, ball, and box objects. Plots (a)-(c) show tracking curves (orange is the object position, blue is the object reference), plots (d)-(f) show position error, and plots (g)-(i) show orientation error.

each parameter set excludes physically impossible values. For example, the object mass parameter set interval contains only positive values. In practice, the size of the parameter sets should be determined by the confidence in the model parameter estimates. Finally, in view of the distributed nature of the proposed algorithm, each agent has information only regarding its own and the object's parameter set. The latter can be defined and distributed to all agents a priori.

The controller gains used in these demonstrations are: $K = 10.0$, $K_v = 5.0$, $A = I_{l_z \times l_z}$, $\Gamma = 0.001 I_{l \times l}$, $\Gamma_o = 0.001 I_{l_o \times l_o}$ with the event triggering constants: $\delta_c = 2.2 \times 10^{-6}$, $\varepsilon_c = 0.001$. The term k_2 is computed at the start of the grasp for which we assume the eigenvalue of G will not deviate too much during the manipulation. Thus we compute: $k_2 = \lambda_{\min}(G_{k=0} G_{k=0}^T K_v) - 1 \times 10^{-7}$. The term c_2 is then computed as $c_2 = \min\{k_1, k_2\} - 1 \times 10^{-7}$. From these constants, the event-triggered conditions (21), (22), and (23) are computed online. The ε constants for the hex, ball, and box objects are respectively $\varepsilon = 3.6$, $\varepsilon = 9.7$, $\varepsilon = 4.0$.

The internal force control from Lemma 4 was applied to the ball and hex objects as they satisfy the symmetry requirement, i.e., the initial contact points were placed equidistantly on the objects. Although the hex object is not spherical, a sphere can be inscribed inside the contact points and satisfy the properties of Lemma 4. The radius of the ball and the hexagon's inscribed sphere is 11cm and 7cm, respectively, resulting in the respective gains of $\frac{\varepsilon}{r\mu} = 75.0$ and $\frac{\varepsilon}{r\mu} = 28.0$. The box was implemented with the internal force control from (11).

A. Comparison Amongst Objects

To demonstrate the applicability of our controller to all objects, we focused on a common manipulation motion where the object must be lifted and lowered along the z-axis. This allows for picking up/dropping off objects in a warehouse and is an in-formation manipulation that cannot be achieved via simple robot formation control since the direction of motion is outside the plane of the bases. For each object, the controller is implemented to track a time-varying, periodic sigmoid signal for translating about the z-axis. We also note that while the z-position is meant to track the periodic reference, the remaining 5 states should not move. Figure 4 shows the proposed control for all objects for the z-translation tracking task. The plots shows similar performance of the proposed controller across all objects, despite their varying size, shape, and mass.

B. Effect of Event-triggering

Next, we investigate the effect of the event-triggering component, γ, on the performance of the system. Recall that γ provides a trade-off of how close the system will track the

reference and how much communication is required to do so. We implement the proposed controller on the ball with the same z-translation task as in Section IV-A, and experiment with different values of γ.

Figure 5 shows the effect of varying γ on the proposed control and Table II shows the associated total number of events and average inter-event time for each value of γ. As expected, the results show an inverse relationship between communication events and magnitude of γ. The plots show that there is no perceivable change in performance as γ increases. This shows that increased communication is *not* needed to achieve the same level of performance and highlights how the event-triggered control law helps reduce communication requirements with minimal impact on performance. We note that the results presented in Theorem 1 provide a worst-case bound as a function of γ, however the other events (21) and (22) can also be triggered, which could improve the performance (see Remark 3). These results indicate that the rolling effects are triggering sufficiently to improve upon the worst-case bound to yield nearly identical performance despite increasing values of γ, yet still reducing the communication requirements.

The effect of (21) and (22) can be seen for $\gamma = 1$, which is associated with the least amount of communication. The gap in communication occurs when the reference trajectory is relatively unchanging at the peaks and troughs. Intuitively, when the reference signal is relatively constant and the object is within the appropriate bound of the error, the event-triggering conditions are satisfied and no communication is required. This highlights another advantage of the proposed method: during lift-and-hold tasks, the agents can exhibit nearly completely decentralized implementation, i.e, without inter-agent communication, once the object is lifted to the desired altitude.

TABLE II: Number of event triggers during manipulation

γ	**Total # of Events**	**Avg. Inter-Event Time (s)**
1.0	373	0.1443
0.1	926	0.0579
0.01	2677	0.0205
0.005	3249	0.0169

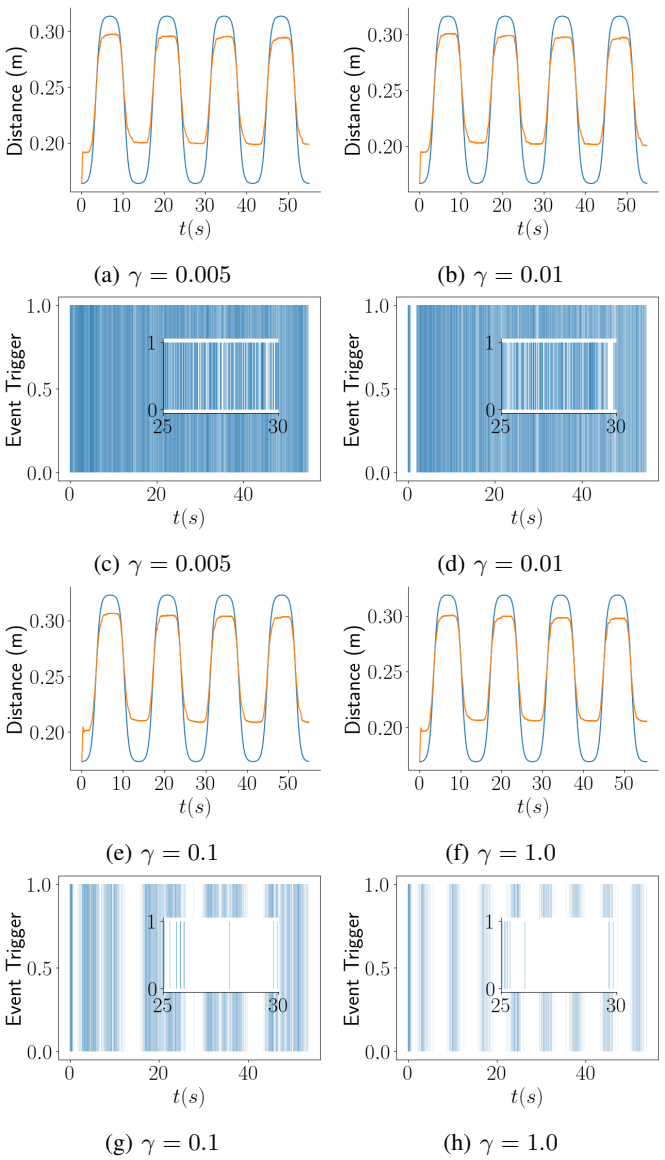

Fig. 5: Comparison of trajectories for different values of γ. The 'Event Trigger' plots show vertical blue lines at each time instant at which an event occurs.

C. Transport Task

In this final demonstration, we show how the proposed control algorithm can be combined with standard formation controllers [28] to provide a distributed solution to transport a ball while avoiding collisions in the environment. The proposed control is implemented as described at the end of Section III where the bases are controlled using standard formation controllers to maintain their initial formation shape. The environment is shown in Figure 6 where the cones define the boundary of the environment. The agents must transport the object from the initial location to the bin, while navigating around an obstacle located at the bend in the L-shaped environment. Furthermore, the bin is located at the boundary of the environment where the agents are not allowed to cross.

To accomplish the aforementioned task, we design a reference trajectory for the agent formation and the manipulators. The formation trajectory translates through the environment and rotates the formation about the obstacle to prevent collision with the obstacle. Similarly, the manipulator trajectory lifts the object above the obstacle to prevent collision. Additionally, the manipulator trajectory is required to translate the object to the bin when the formation can no longer traverse the distance to the goal due to the boundary of the environment. The error trajectories associated with the position and orientation for the transport task are shown in Figure 7. A video of the demonstration can be found in [31], and depicts the object successfully transported to the goal location, while avoiding the obstacle and remaining within the boundary region.

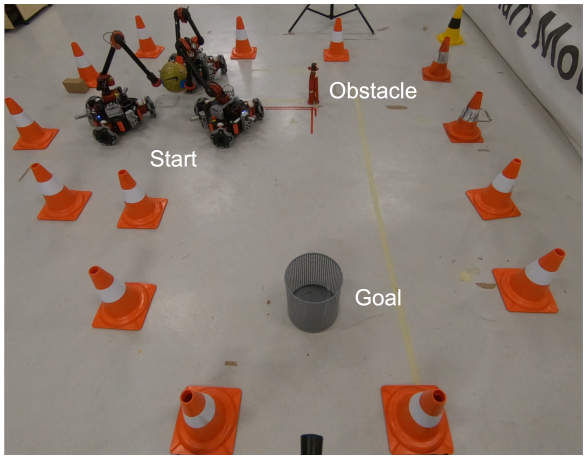

Fig. 6: Transport environment with start, goal, and obstacle.

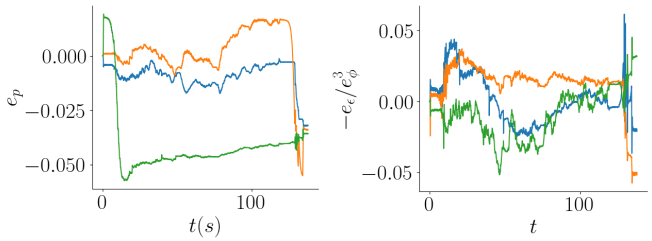

Fig. 7: Position and orientation errors for transport task demonstration.

V. Conclusion

In this paper we present a novel, event-triggered, adaptive control scheme for multi-agent cooperative manipulation with rolling contacts. The event-triggering component allows for distributed control in the sense that agents update each others contact information only as needed and the control (including determination of events) is computed by each agent independently. The proposed controller ensures ultimate boundedness trajectory tracking, while actively preventing slip. Furthermore, the proposed controllers are robust to uncertainty in the object mass and are not dependent on the rigidity assumption, which allows for grasping more general objects than can be held with grippers. Hardware implementation demonstrates the effectiveness of the proposed method. Future work will incorporate multi-agent grasp formation/re-grasping and time-varying base formation for robot swarms.

VI. Acknowledgements

The authors would like to thank Gil Serrano and Robin Baran for their help in setting up and implementing the robots and experiments.

VII. Appendix

Proof of Theorem 1. The proof is structured into two Cases. Case 1 addresses the system if no event occurs. Case 2 addresses if an event occurs and ensures non-Zeno behaviour for the time updates. We first note that Assumptions 1 -3 ensure that (17) and (11) are well-defined.

Case 1: Here we address the system if no event occurs, i.e., $t_k = 0$, $t_{k+1} = \infty$. Next, note by (2), (3), and (12) that, when $\boldsymbol{f}_{c_i}^{C_i} \in \mathring{\mathcal{F}}_{c_i}$, each $\boldsymbol{f}_{c_i}^{C_i}$ can be written as a function of the stack state, i.e., $\boldsymbol{f}_{c_i}^{C_i} = \boldsymbol{f}_{c_i}^{C_i}(\boldsymbol{\chi})$, for all $i \in \mathcal{N}$. Consider also the set

$$\mathcal{U} := \{\boldsymbol{\chi} \in \mathcal{X} : \|\frac{\boldsymbol{e}_\epsilon}{e_\phi}\| < \bar{e}_\epsilon, \|\boldsymbol{e}_p\| < \bar{e}_p, \|\boldsymbol{e}_v\| < \bar{e}_v, \\ \|\boldsymbol{e}_\nu\| < \tilde{e}_\nu, \|\boldsymbol{e}_{\nu_o}\| < \tilde{e}_{\nu_o}, \boldsymbol{f}_{c_i}^{C_i}(\boldsymbol{\chi}) \in \text{Int}(\mathring{\mathcal{F}}_{c_i}), \forall i \in \mathcal{N}\},$$

for some positive constants $\bar{e}_\epsilon > 1$, $\bar{e}_v$, $\bar{e}_p$ satisfying $\|\boldsymbol{e}_v(0)\| < \bar{e}_v$, $\|\boldsymbol{e}_p(0)\| < \bar{e}_p$, and $\tilde{e}_\nu, \tilde{e}_{\nu_o}$ larger than $\bar{e}_\nu, \bar{e}_{\nu_o}$, respectively, which were introduced in (20). Next, by using (17) and (18), one obtains the closed-loop dynamics $\dot{\boldsymbol{\chi}} = \boldsymbol{h}_\chi(\boldsymbol{\chi}, t)$, where $\boldsymbol{h}_\chi : \mathcal{X} \times \mathbb{R}_{\geq 0} \to \mathcal{X}$ is a function that is continuous in t and locally Lipschitz in $\boldsymbol{\chi}$. Note that $\boldsymbol{\chi}(0) \in \mathcal{U}$. Then, according to Theorem 2.1.3 of [32], there exists a positive time constant $\tau > 0$ and a unique solution $\boldsymbol{\chi} : [0, \tau) \to \mathcal{U}$, i.e., defined for $[0, \tau)$ and satisfying $\boldsymbol{\chi}(t) \in \mathcal{U}$, for all $t \in [0, \tau)$. Hence, slip does not occur and the dynamics (13) are well-defined, for $t \in [0, \tau)$. Let now a candidate Lyapunov function be

$$V := \frac{1}{2}\|\boldsymbol{e}_p\|_2^2 + \frac{\|\boldsymbol{e}_\varepsilon\|_2^2}{e_\phi^2} + \frac{1}{2}\boldsymbol{e}_v^\top \tilde{M}\boldsymbol{e}_v + \frac{1}{2}\boldsymbol{e}_\nu^\top \Gamma^{-1}\boldsymbol{e}_\nu + \frac{1}{2}\boldsymbol{e}_{\nu_o}^\top \Gamma_o^{-1}\boldsymbol{e}_{\nu_o} \tag{28}$$

Since $e_\varphi(0) \neq 0$, it holds that $V|_{t=0} \leq \bar{V}_0$ for a bounded $\bar{V}_0 \in \mathbb{R}_{>0}$. Also, by properties of the unit quaternion, it holds that $\frac{1}{e_\phi^2} - 1 = \frac{\|\boldsymbol{e}_\varepsilon\|_2^2}{e_\phi^2}$.

Differentiation of V results in:

$$\dot{V} = \boldsymbol{e}^\top(\boldsymbol{v}_o - \boldsymbol{v}_\text{d}) + \frac{1}{2}\boldsymbol{e}_v^\top \dot{\tilde{M}}\boldsymbol{e}_v + \boldsymbol{e}_v^\top(-\tilde{C}\boldsymbol{v}_o - \tilde{\boldsymbol{g}} - \tilde{M}\dot{\boldsymbol{v}}_f \\ + GJ_h^{-T}\boldsymbol{u}) + \boldsymbol{e}_\nu^\top \Gamma^{-1}\dot{\boldsymbol{e}}_\nu + \boldsymbol{e}_{\nu_o}^\top \Gamma_o^{-1}\dot{\boldsymbol{e}}_{\nu_o}$$

which, after substitution of (17), becomes

$$\dot{V} = -\boldsymbol{e}^\top K\boldsymbol{e} - \boldsymbol{e}_v^\top GG^\top K_v\boldsymbol{e}_v + \boldsymbol{e}_v^\top GG_k^* Y_{o_r}\hat{\boldsymbol{\nu}}_o - \boldsymbol{e}_v^\top Y_{o_r}\boldsymbol{\nu}_o \\ - \boldsymbol{e}_v^\top(GG_k^* - I)\boldsymbol{e} + \boldsymbol{e}_v^\top G\boldsymbol{f}_{\text{int}_k} + \boldsymbol{e}_{\nu_o}^\top \Gamma_o^{-1}\dot{\hat{\boldsymbol{\nu}}}_o$$

From $\Delta G = G - G_k$ it follows that $GG_k^* - I_{6\times 6} = \Delta GG_k^*$ which yields, along with (18), (19), and the fact that $G_k\boldsymbol{f}_{\text{int}_k} = \boldsymbol{0}$:

$$\dot{V} \leq -k_1\|\boldsymbol{e}\|^2 - k_2\|\boldsymbol{e}_v\|^2 + \boldsymbol{e}_v^\top \Delta GG_k^* Y_{o_r}\hat{\boldsymbol{\nu}}_o - \boldsymbol{e}_v^\top \Delta GG_k^*\boldsymbol{e} \\ + \boldsymbol{e}_v\Delta G\boldsymbol{f}_{\text{int}_k}$$

Note that k_2 can be increased by tuning K_v. From $\Delta G_i = \begin{bmatrix} 0_{3\times 3} \\ (\Delta\boldsymbol{p}_{oc_i})\times \end{bmatrix}$ and $\Delta G = [\Delta G_1, ..., \Delta G_N]$, it follows that $\|\Delta GG_k^*\| \leq \|\Delta G\|\|G_k^*\| \leq \sum_i \|\Delta\boldsymbol{p}_{oc_i}\|\|G_{k_i}^*\|$. From the triggering condition (24), it follows that $\|\Delta\boldsymbol{p}_{oc_i}\| \leq \delta_p$ for all $i \in \mathcal{N}$. We thus define $c_1 := \delta_p \sum_i \|G_{k_i}^*\|$, which is constant between events, such that $\|\Delta GG_k^*\| \leq c_1$. Note that Assumptions 1 and 3 as well as the fact that slip does not occur for $[0, \tau)$ imply that $\|\Delta GG_k^*\|$ is well defined and bounded, for all $i \in \mathcal{N}$. Hence, $\dot{V}$ becomes

$$\dot{V} \leq -k_1\|\boldsymbol{e}\|^2 - k_2\|\boldsymbol{e}_v\|^2 + \boldsymbol{e}_v^\top \Delta GG_k^* Y_{o_r}\hat{\boldsymbol{\nu}}_o + c_1\|\boldsymbol{e}_v\|\|\boldsymbol{e}\| \\ + \boldsymbol{e}_v\Delta G\boldsymbol{f}_{\text{int}_k}$$

We then complete the squares such that $c_1\|\boldsymbol{e}_v\|\|\boldsymbol{e}\| \leq \frac{c_1}{2}\|\boldsymbol{e}_v\|^2 + \frac{c_1}{2}\|\boldsymbol{e}\|^2$, which leads to

$$\dot{V} \leq -\left(k_1 - \frac{c_1}{2}\right)\|\boldsymbol{e}\|^2 - \left(k_2 - \frac{c_1}{2}\right)\|\boldsymbol{e}_v\|^2 + \boldsymbol{e}_v^\top \Delta G G_k^* Y_{o_r} \hat{\boldsymbol{\nu}}_o + \boldsymbol{e}_v \Delta G \boldsymbol{f}_{\text{int}_k}$$

We introduce now a constant $c_2 \in \mathbb{R}_{>0}$ such that:

$$\begin{aligned}\dot{V} \leq& -\left(k_1 - \frac{c_1}{2} - c_2\right)\|\boldsymbol{e}\|^2 - \left(k_2 - \frac{c_1}{2} - c_2\right)\|\boldsymbol{e}_v\|^2 \\ &- c_2\|\boldsymbol{e}\|^2 - c_2\|\boldsymbol{e}_v\|^2 + \boldsymbol{e}_v^\top \Delta G G_k^* Y_{o_r} \hat{\boldsymbol{\nu}}_o + \boldsymbol{e}_v \Delta G \boldsymbol{f}_{\text{int}_k} \\ =:& -(k_e - c_2)\|\boldsymbol{e}\|^2 - (k_{e_v} - c_2)\|\boldsymbol{e}_v\|^2 - c_2\|\boldsymbol{e}\|^2 - c_2\|\boldsymbol{e}_v\|^2 \\ &+ \boldsymbol{e}_v^\top \Delta G G_k^* Y_{o_r} \hat{\boldsymbol{\nu}}_o + \boldsymbol{e}_v \Delta G \boldsymbol{f}_{\text{int}_k}\end{aligned}$$

where $k_e \coloneqq k_1 - \frac{c_1}{2}$ and $k_{e_v} \coloneqq k_2 - \frac{c_1}{2}$. Note that since (21) is satisfied, $k_e > c_2$ and $k_{e_v} > c_2$, for c_2 from (23).

Let $\mathcal{Q} \coloneqq \{\boldsymbol{\chi} \in \mathcal{X} : \|\boldsymbol{e}\|^2 + \|\boldsymbol{e}_v\|^2 \leq \gamma\}$. Note that $\mathcal{Q}$ is compact since $\boldsymbol{e}_\nu$, $\boldsymbol{e}_{\nu_o}$ are bounded as per (20). Choose $\rho_\gamma = \max V(\boldsymbol{\chi}) s.t. \boldsymbol{\chi} \in \partial\mathcal{Q}$ and let $\Omega_{\rho_\gamma} \coloneqq \{\boldsymbol{\chi} \in \mathcal{X} : V(\boldsymbol{\chi}) \leq \rho_\gamma\}$ Moreover, in $\mathcal{X}\backslash\mathcal{Q}$ and in $\mathcal{X}\backslash\Omega_{\rho_\gamma}$, it holds that $\|\boldsymbol{e}\|^2 + \|\boldsymbol{e}_v\|^2 > \gamma$ and hence $c_2\|\boldsymbol{e}\|^2 + c_2\|\boldsymbol{e}_v\|^2 > c_2\gamma$, and $\dot{V}$ becomes

$$\begin{aligned}\dot{V} \leq& -(k_e - c_2)\|\boldsymbol{e}\|^2 - (k_{e_v} - c_2)\|\boldsymbol{e}_v\|^2 \\ &+ \boldsymbol{e}_v^\top \Delta G G_k^* Y_{o_r} \hat{\boldsymbol{\nu}}_o + \boldsymbol{e}_v \Delta G \boldsymbol{f}_{\text{int}_k} - c_2\gamma\end{aligned}$$

According to (23), the following condition holds between events

$$\boldsymbol{e}_v^\top \begin{bmatrix} 0_{3\times 3} \\ (\Delta \boldsymbol{p}_{oc_i})\times \end{bmatrix} \left(\boldsymbol{f}_{\text{int}_{k,i}} + G_{k_i}^* Y_{or} \hat{\boldsymbol{\nu}}_o\right) - c_2\gamma \leq 0. \quad (29)$$

By summing for all $i \in \mathcal{N}$, the latter becomes

$$\boldsymbol{e}_v^\top \Delta G G_k^* (Y_{or} \hat{\boldsymbol{\nu}}_o + \boldsymbol{f}_{\text{int}_k}) - c_2\gamma \leq 0,$$

implying that $\dot{V} \leq -(k_e - c_2)\|\boldsymbol{e}\|^2 - (k_{e_v} - c_2)\|\boldsymbol{e}_v\|^2 < 0$. By following the standard results (e.g., see proof of Theorem 4.18 of [33]), it can be shown that $\chi(t)$ will reach Ω_{ρ_γ} in finite time and Ω_{ρ_γ} is an invariant set so that there exists a T_1 such that $\|\boldsymbol{e}\|^2 + \|\boldsymbol{e}_v\|^2 \leq \rho_\gamma$ for all $t \geq T_1$.

By using (20), we now investigate $\dot{V}$ inside Ω_{ρ_γ}, for which it holds $\|\boldsymbol{e}_v\| \leq \frac{2\sqrt{\rho_\gamma}}{\lambda_{M_{min}}}$, where $\lambda_{M_{min}} > 0$ is the minimum eigenvalue of the positive-definite matrix $\tilde{M}$ for all $\boldsymbol{\chi} \in \Omega_{\rho_\gamma}$:

$$\begin{aligned}\dot{V} \leq& -k_e\|\boldsymbol{e}\|^2 - k_{e_v}\|\boldsymbol{e}_v\|^2 + \boldsymbol{e}_v^\top \Delta G G_k^* Y_{o_r} \hat{\boldsymbol{\nu}}_o + \boldsymbol{e}_v \Delta G \boldsymbol{f}_{\text{int}_k} \\ \leq& -k_e\|\boldsymbol{e}\|^2 - k_{e_v}\|\boldsymbol{e}_v\|^2 - \beta_\nu\|\boldsymbol{e}_\nu\|^2 - \beta_{\nu_o}\|\boldsymbol{e}_{\nu_o}\|^2 + \beta_\nu \bar{e}_\nu^2 \\ &+ \beta_{\nu_o}\bar{e}_{\nu_o}^2 + \boldsymbol{e}_v^\top \Delta G G_k^* Y_{o_r} \boldsymbol{e}_{\nu_o} + \boldsymbol{e}_v^\top \Delta G G_k^* Y_{o_r} \boldsymbol{\nu}_o \\ &+ \boldsymbol{e}_v^\top \Delta G \boldsymbol{f}_{\text{int}_k} \\ \leq& -k_e(\|\boldsymbol{e}_p\|^2 + \frac{\|\boldsymbol{e}_\varepsilon\|^2}{e_\phi^2}) - k_{e_v}\|\boldsymbol{e}_v\|^2 - \beta_\nu\|\boldsymbol{e}_\nu\|^2 - \beta_{\nu_o}\|\boldsymbol{e}_{\nu_o}\|^2 \\ &+ \beta_\nu \bar{e}_\nu^2 + \beta_{\nu_o}\bar{e}_{\nu_o}^2 + \frac{2\sqrt{\rho_\gamma}}{\lambda_{M_{min}}}\|\Delta G G_k^*\|\|Y_{o_r}\|\bar{e}_{\nu_o} \\ &+ \frac{2\sqrt{\rho_\gamma}}{\lambda_{M_{min}}}\|\Delta G G_k^*\|\|Y_{o_r}\|\|\boldsymbol{\nu}_o\| + \frac{2\sqrt{\rho_\gamma}}{\lambda_{M_{min}}}\|\Delta G\|\|\boldsymbol{f}_{\text{int}_k}\|,\end{aligned}$$

where β_ν, $\beta_{\nu_o} \in \mathbb{R}_{>0}$ are positive constants. Note that in the previous inequality, $-\|\boldsymbol{e}\|^2 = -\|\boldsymbol{e}_p\|^2 - \frac{\|\boldsymbol{e}_\varepsilon\|^2}{e_\phi^6} \leq -\|\boldsymbol{e}_p\|^2 - \frac{\|\boldsymbol{e}_\varepsilon\|^2}{e_\phi^2}$ since $e_\phi^4 \leq 1$ and so $-\frac{a}{e_\phi^4} \leq -a$ for any $a > 0$. Since $\|\Delta G G_k^*\| \leq \|\Delta G\|\|G_k^*\| \leq c_1$, it holds that $\|\Delta G\| \leq \frac{c_1}{\|G_k^*\|}$, which is bounded, since $\sigma_{\min}(G_k^*) = \frac{1}{\sigma_{\max}(G_k)}$ and G_k is full row rank. Furthermore, $\boldsymbol{f}_{\text{int}_k}$ is constant between events. Thus, in view of (20) and since χ lies in the compact set Ω_{ρ_γ}, we can conclude that there exists a $\bar{\delta}_k$ such that:

$$\begin{aligned}\bar{\delta}_k \geq& \beta_\nu \bar{e}_\nu^2 + \beta_{\nu_o}\bar{e}_{\nu_o}^2 + \frac{2\sqrt{\rho_\gamma}}{\lambda_{M_{min}}}\|\Delta G G_k^*\|\|Y_{o_r}\|\bar{e}_{\nu_o} \\ &+ \frac{2\sqrt{\rho_\gamma}}{\lambda_{M_{min}}}\|\Delta G G_k^*\|\|Y_{o_r}\|\|\boldsymbol{\nu}_o\| + \frac{2\sqrt{\rho_\gamma}}{\lambda_{M_{min}}}\|\Delta G\|\|\boldsymbol{f}_{\text{int}_k}\|\end{aligned} \quad (30)$$

Hence $\dot{V}$ becomes

$$\dot{V} \leq -k_\chi\|\boldsymbol{\chi}\|^2 + \bar{\delta}_k,$$

where $k_\chi \coloneqq \min\{k_e, k_{e_v}, \beta_\nu, \beta_{\nu_o}\}$. Since V is positive-definite, there exist class-$\mathcal{K}$ functions α_1, α_2, such that $\alpha_1(\|\boldsymbol{\chi}\|) \leq V(\boldsymbol{\chi}) \leq \alpha_2(\|\boldsymbol{\chi}\|)$. Therefore, by invoking [33, Th. 4.18], we guarantee that $\boldsymbol{\chi}$ is ultimately bounded in a compact set defined by k_χ and $\bar{\delta}_k$, for $t \in [0, \tau)$. Note that the size of this compact set is proportional to k_e, k_{e_v}, and γ.

Now we investigate the slip prevention properties. By using (2), (7) and (12), one obtains the following expression for the interaction forces: $\boldsymbol{f}_c = B^{-1}\Big(J_h M^{-1}\Big[\boldsymbol{u}_k - \boldsymbol{g} - \Big(CJ_h^{-1}G^\top + M\frac{d}{dt}(J_h^{-1}G^\top)\Big)\boldsymbol{v}_o\Big] + G^\top M_o^{-1}(C_o\boldsymbol{v}_o + \boldsymbol{g}_o)\Big)$, where $B \coloneqq J_h M^{-1} J_h^\top + G^\top M_o^{-1} G$. We substitute (17) for $\boldsymbol{u}_k$, $\boldsymbol{v}_f = \boldsymbol{e}_v + \boldsymbol{v}_o$ and (14), and add and subtract $B^{-1}G^\top M_o^{-1} G G_k^* \boldsymbol{f}_d$ and $B^{-1}G^\top M_o^{-1} G \boldsymbol{f}_{\text{int}_k}$ to obtain:

$$\boldsymbol{f}_c = (I - B^{-1}G^\top M_o^{-1}\Delta G)\boldsymbol{f}_{\text{int}_k} + \boldsymbol{h}_k \quad (31)$$

$$\begin{aligned}\boldsymbol{h}_k \coloneqq& \boldsymbol{\lambda}_k + B^{-1}J_h M^{-1}(Y_r\hat{\boldsymbol{\nu}} - Y\boldsymbol{\nu}) + \\ &B^{-1}G^\top M_o^{-1}\Big(GG^\top K_v \boldsymbol{e}_v + \boldsymbol{e} + Y_o\boldsymbol{\nu}_o - Y_{o_r}\hat{\boldsymbol{\nu}}_o \\ &+ \Delta G G_k^*(\boldsymbol{e} - Y_{o_r}\hat{\boldsymbol{\nu}}_o)\Big)\end{aligned} \quad (32)$$

Substitution of $\boldsymbol{f}_c$ into (10), which is the condition for slip prevention, yields the following condition to be satisfied:

$$\Lambda(\mu)R_{pc}^\top(I - B^{-1}G^\top M_o^{-1}\Delta G)\boldsymbol{f}_{\text{int}_k} \succeq -\Lambda(\mu)R_{pc_k}^\top \boldsymbol{h}_k$$

From the boundedness of signals, we conclude that $\boldsymbol{h}_k$ is bounded for all $t \in [0, \tau)$ in a compact set, independent of τ. Let now ε_h denote the maximum bound of the elements of $\pm\Lambda(\mu)R_{pc_k}^\top \boldsymbol{h}_k$ and substitute $\boldsymbol{f}_{\text{int}_k} = R_{pc_k}\boldsymbol{\ell}_k^*$ with $W \coloneqq (R_{pc}^\top R_{pc_k} - I_{3N\times 3N}) - R_{pc}^\top B^{-1}G^\top M_o^{-1}\Delta G R_{pc_k}$ to re-write the sufficient condition for no slip as:

$$\Lambda(\mu)(I - W)\boldsymbol{\ell}_k^* \succeq \varepsilon_h \mathbf{1} \quad (33)$$

Here we show that (22) and (21) ensure that $\|W\|_\infty \leq \delta_c$. By the boundedness of the system dynamics and rotation matrices, there exist $g_1, g_2 \in \mathbb{R}_{\geq 0}$ such that $\|R_{pc_k}\|_\infty \leq \|R_{pc}\|_\infty \leq g_1$ and $\|R_{pc}^\top B^{-1}G^\top M_o^{-1}\| \leq g_2$. Furthermore, the structure of G yields: $\|\Delta G\|_\infty \leq \sum_i \|\Delta \boldsymbol{p}_{oc_i}\|_1$. By the equivalence

of norms and (21), there exists a $g_3 \in \mathbb{R}_{>0}$ such that $\sum_i \|\Delta \boldsymbol{p}_{oc_i}\|_1 \leq g_3 N \delta_r$ such that $\|\Delta G\|_\infty \leq g_3 N \delta_p$. From the block diagonal structure of R_{pc} we can also compute $\|R_{pc}^\top R_{pc_k} - I_{3N\times 3N}\|_\infty \leq \max_i \|R_{pc_i}^\top R_{pc_{k,i}} - I_{3\times 3}\|_\infty$. Again, by the equivalence of norms and (22) there exists a $g_4 \in \mathbb{R}_{>0}$ such that: $\|R_{pc_i}^\top R_{pc_{k,i}} - I_{3\times 3}\|_\infty \leq g_4 \delta_r$. Now we can upper bound W using the triangle inequality: $\|W\|_\infty \leq \|R_{pc}^\top R_{pc_k} - I_{3N\times 3N}\|_\infty + \|R_{pc}^\top B^{-1} G^\top M_o^{-1}\|_\infty \|R_{pc_k}\|_\infty \|\Delta G\|_\infty \leq g_1 g_4 \delta_r + g_2 g_1 g_3 N \delta_p \leq \max\{g_1 g_4, g_2 g_1 g_3 N\}(\delta_r + \delta_p)$. Now for sufficiently large $\varepsilon_c \geq \max\{g_1 g_4, g_2 g_1 g_3 N\}$, $\|W\|_\infty \leq \varepsilon_c(\delta_r + \delta_p)$. Since $\delta_r < \frac{\delta_c}{2\varepsilon_c}$ and $\delta_p < \frac{\delta_c}{2\varepsilon_c}$ it holds that $\|W\|_\infty \leq \delta_c$.

Next, by Assumption 2, there exists an $\|\boldsymbol{\ell}\|_2 \leq \bar{l}$ satisfying (11). Furthermore, since the solution of (11) minimizes $\|\boldsymbol{\ell}\|_2$, then $\|\boldsymbol{\ell}_k^*\|_2 \leq \bar{l}$ must hold. We note that by equivalence of norms, the following also holds: $\|\boldsymbol{\ell}_k\|_\infty \leq \|\boldsymbol{\ell}_k\|_2 \leq \bar{l}$. Now for ε chosen large enough such that $\varepsilon \geq \varepsilon_h + \lambda \delta_c \bar{l}$, (11) ensures $\Lambda(\mu)\boldsymbol{\ell}_k^* \succeq (\varepsilon_h + \lambda \delta_c \bar{l})\mathbf{1}_{3N}$. Lemma 1 then ensures that (33) holds and hence contact slip is actively prevented $\forall t \in [0, \tau)$. In fact, the internal forces analysis above and the fact that Λ defines pyramid constraints imply that $\boldsymbol{f}_{c_i}^{\mathcal{C}_i} \in \bar{\mathcal{F}}_{c_i}$, where $\bar{\mathcal{F}}_{c_i}$ is a compact subset of $\text{Int}(\mathcal{F}_{c_i})$, $\forall i \in \mathcal{N}$. Therefore, since $\boldsymbol{e}_\nu$ and $\boldsymbol{e}_{\nu_o}$ are uniformly bounded through the projection operator by $\bar{e}_\nu$ and $\bar{e}_{\nu_o}$, respectively, by choosing large enough $\bar{e}_p$ and $\bar{e}_v$ in the definition of $\mathcal{U}$, $\chi(t)$ belongs to a compact subset $\bar{\mathcal{U}}$ of $\mathcal{U}$, $\forall t \in [0, \tau)$. Thus by invoking the maximal solutions' theorem (e.g., Th. 2.1.4 of [32]), it follows that $\tau \to \infty$. Thus slip prevention and ultimate-boundedness is ensured, which yields (26) and (27) for $\bar{\delta} = \bar{\delta}_k$.

Case 2: Here we show that the event triggering preserves the results from Case 1 and ensure no Zeno behaviour.

First we show that there exists a lower bound between two consecutive triggering time instants. Events (21) and (22) are dependent on bounds δ_r and δ_p, where $\delta_r > 0$ is fixed and $\delta_p > 0$ and will never tend to zero due to boundedness of $\boldsymbol{p}_{oc_i}$ such that $\|G_{i,k}^*\|$ will not tend to infinity (recall that all signals have been shown to be bounded). From the Lipschitz continuity of $\boldsymbol{p}_{oc_i}$ and R_{pc_i}, and the system's states, let $L_p, L_r \in \mathbb{R}_{>0}$ denote the respective Lipschitz constants with respect to time such that $\|\boldsymbol{p}_{oc_i}(t_p) - \boldsymbol{p}_{oc_i}(t_k)\| \leq L_p(t_p - t_k)$ and $\|f_r(t_r) - f_r(t_k)\| \leq L_r(t_r - t_k)$ for $f_r(t) = I_{3\times 3} - R_{pc_i}(t)^\top R_{pc_{k,i}}$. In the worst case, suppose these terms achieve their Lipschitz upper bounds and trigger the event such that $\|\boldsymbol{p}_{oc_i}(t_p) - \boldsymbol{p}_{oc_i}(t_k)\| = L_p(t_p - t_k) = \delta_p$ and $\|f_r(t_r) - f_r(t_k)\| = L_r(t_r - t_k) = \delta_r$ which yields $\Delta t_p = t_p - t_k = \frac{\delta_p}{L_p} > 0$ and $\Delta t_r = t_r - t_k = \frac{\delta_r}{L_r} > 0$.

Similarly, the event defined by (23) depends on the bound $c_2\gamma$. Denote by $\boldsymbol{e}_v \coloneqq [\boldsymbol{e}_{v_p}^\top, \boldsymbol{e}_{v_\eta}^\top]^\top \in \mathbb{R}^3 \times \mathbb{R}^3$. Let $f_e(t) = \boldsymbol{e}_{v_\eta}(t)^\top(\Delta \boldsymbol{p}_{oc_i}(t)) \times \boldsymbol{f}_{\text{int}_{i_k}} + G_{k_i}^* Y_{o_r}(t)\hat{\boldsymbol{\nu}}_o(t)$. Using the same argument with Lipschitz continuity of f_e yields the following relation in the worst case when the Lipschitz constant bound is reached: $\|f_e(t_{k+1}) - f_e(t_k)\| = L_e(t_{k+1} - t_k) =: L_e \Delta t_e = c_2\gamma$, such that $\Delta t_e = \frac{L_e}{c_2\gamma} > 0$.

Finally, as t_k is defined by satisfaction of any events from (21), (22), or (23), it follows that $\Delta t \coloneqq t_{k+1} - t_k = \min\{\frac{\delta_p}{L_p}, \frac{\delta_r}{L_r}, \frac{L_e}{c_2\gamma}\}$ where $\Delta t > 0$ and lower bounded. We note that the event-triggering introduces a discontinuous jump in the control. However, since Δt is lower bounded, the events, and thus the step discontinuity in the control, occur on a set of measure zero. From Caratheodory's Theorem [34], the solution $\boldsymbol{\chi}(t)$ is absolutely continuous.

Now consider the analysis of Case 1 if events do occur. First, as with the solution of $\boldsymbol{\chi}(t)$, $V(\boldsymbol{\chi}(t), t)$ is absolutely continuous during events such that $\dot{V}$ exists almost everywhere on $t \in [t_k, t_{k+1}]$. Now consider $V_k = \lim_{t \to t_k} V(\boldsymbol{\chi}(t), t)$. Also, at $t = t_k$, the agents communicate such that $\Delta \boldsymbol{p}_{oc} = 0$, $\Delta G = 0$, $\|R_{pc}\top R_{pc_k} - I_{3N\times 3N}\| = 0$. So at each event, the conditions of Case 1 are satisfied and so the analysis can be repeated for $t \in [t_k, t_{k+1})$ with the initial condition $V = V_k$ for $\dot{V}$. Also, $t = t_k$, $W = 0$ such that the no slip condition holds following the same analysis as in Case 1. For $\chi \in \Omega_{\rho_\gamma}$, the condition $\dot{V} \leq k_\chi \|\chi\|^2 + \bar{\delta}_k$ holds although $\bar{\delta}_k$ will change between events. However, since χ and $\boldsymbol{f}_{\text{int}_k}$ are bounded in Ω_{ρ_γ}, there exists a maximum $\bar{\delta} \geq \bar{\delta}_k$ for all $k \in \mathbb{N}$. The analysis of Case 1 can be repeated by induction between all events as $t \to \infty$, and thus the ultimate boundedness of the system and no slip condition, $\boldsymbol{f}_c^{\mathcal{C}_i}(t) \in \mathcal{F}_{c_i}$ holds for all $t \geq 0$, $i \in \mathcal{N}$ which yields (26) and (27).

□

REFERENCES

[1] S. Erhart, D. Sieber, and S. Hirche, "An impedance-based control architecture for multi-robot cooperative dual-arm mobile manipulation," *IEEE/RSJ International Conference on Intelligent Robots and Systems (IROS)*, pp. 315–322, 2013.

[2] F. Ficuciello, A. Romano, L. Villani, and B. Siciliano, "Cartesian impedance control of redundant manipulators for human-robot co-manipulation," *IEEE/RSJ International Conference on Intelligent Robots and Systems (IROS)*, pp. 2120–2125, 2014.

[3] A.-N. Ponce-Hinestroza, J.-A. Castro-Castro, H.-I. Guerrero-Reyes, V. Parra-Vega, and E. Olguín-Díaz, "Cooperative redundant omnidirectional mobile manipulators: Model-free decentralized integral sliding modes and passive velocity fields," *IEEE International Conference on Robotics and Automation (ICRA)*, pp. 2375–2380, 2016.

[4] Y.-H. Liu and S. Arimoto, "Decentralized adaptive and nonadaptive position/force controllers for redundant manipulators in cooperations," *The International Journal of Robotics Research*, vol. 17, no. 3, pp. 232–247, 1998.

[5] C. K. Verginis, M. Mastellaro, and D. V. Dimarogonas, "Robust cooperative manipulation without force/torque measurements: Control design and experiments," *IEEE Transactions on Control Systems Technology*, 2019.

[6] R. Ozawa and K. Tahara, "Grasp and dexterous manipulation of multi-fingered robotic hands: a review from a control view point," *Advanced Robotics*, vol. 31, no. 19-20, pp. 1030–1050, 2017.

[7] J. Kerr and B. Roth, "Analysis of multifingered hands," *Int. J. Robot. Res.*, vol. 4, no. 4, pp. 3–17, 1986.

[8] A. B. Cole, J. E. Hauser, and S. S. Sastry, "Kinematics and control of multifingered hands with rolling contact," *IEEE Transactions on Automatic Control*, vol. 34, no. 4, pp. 398–404, 1989.

[9] Y. Fan, L. Sun, M. Zheng, W. Gao, and M. Tomizuka, "Robust dexterous manipulation under object dynamics uncertainties," *IEEE International Conference on Advanced Intelligent Mechatronics*, pp. 613–619, 2017.

[10] A. Caldas, A. Micaelli, M. Grossard, M. Makarov, P. Rodriguez-Ayerbe, and D. Dumur, "Object-level impedance control for dexterous manipulation with contact uncertainties using an LMI-based approach," *IEEE International Conference on Robotics and Automation (ICRA)*, pp. 3668–3674, 2015.

[11] T. Wimböck, C. Ott, A. Albu-Schäffer, and G. Hirzinger, "Comparison of object-level grasp controllers for dynamic dexterous manipulation," *The International Journal of Robotics Research*, vol. 31, no. 1, pp. 3–23, 2012.

[12] K. Tahara, S. Arimoto, and M. Yoshida, "Dynamic object manipulation using a virtual frame by a triple soft-fingered robotic hand," in *IEEE International Conference on Robotics and Automation (ICRA)*, 2010, pp. 4322–4327.

[13] A. Kawamura, K. Tahara, R. Kurazume, and T. Hasegawa, "Dynamic grasping of an arbitrary polyhedral object," *Robotica*, vol. 31, no. 4, pp. 511–523, 2013.
[14] W. Shaw Cortez, D. Oetomo, C. Manzie, and P. Choong, "Tactile-based blind grasping: Trajectory tracking and disturbance rejection for in-hand manipulation of unknown objects," *American Control Conference (ACC)*, pp. 693–698, 2019.
[15] S. Ueki, H. Kawasaki, and T. Mouri, "Adaptive control of multi-fingered robot hand using quaternion," in *17th IFAC World Congress*, 2008, pp. 6757–6762.
[16] S. Ueki, H. Kawasaki, T. Mouri, and A. Kaneshige, "Object manipulation based on robust and adaptive control by hemispherical soft fingertips," *18th IFAC World Congress*, vol. 18, pp. 14 654–14 659, 2011.
[17] C. Cheah, H. Han, S. Kawamura, and S. Arimoto, "Grasping and position control for multi-fingered robot hands with uncertain jacobian matrices," in *IEEE International Conference on Robotics and Automation (ICRA)*, vol. 3, 1998, pp. 2403–2408.
[18] W. Shaw Cortez, D. Oetomo, C. Manzie, and P. Choong, "Tactile-based blind grasping: A discrete-time object manipulation controller for robotic hands," *IEEE Robot. Autom. Lett.*, vol. 3, no. 2, 2018.
[19] P. Fungtammasan and T. Watanabe, "Grasp input optimization taking contact position and object information uncertainties into consideration," *IEEE Trans. Robot.*, vol. 28, no. 5, pp. 1170–1177, 2012.
[20] C. K. Verginis, W. Shaw Cortez, and D. V. Dimarogonas, "Adaptive Cooperative Manipulation with Rolling Contacts," in *2020 American Control Conference (ACC)*, 2020, pp. 2735–2740.
[21] R. Murray, Z. Li, and S. Sastry, *A mathematical introduction to robotic manipulation*. CRC Press: Boca Raton, FL, USA, 1994.
[22] A. Cole, J. Hauser, and S. Sastry, "Kinematics and control of multifingered hands with rolling contact," *IEEE Trans. Autom. Control*, vol. 34, no. 4, pp. 398–404, 1989.
[23] V. Lippiello, F. Ruggiero, B. Siciliano, and L. Villani, "Visual Grasp Planning for Unknown Objects Using a Multifingered Robotic Hand," *Ieee-Asme Transactions on Mechatronics*, vol. 18, no. 3, pp. 1050–1059, Jun. 2013.
[24] W. Shaw Cortez, D. Oetomo, C. Manzie, and P. Choong, "Grasp constraint satisfaction for object manipulation using robotic hands," *IEEE Conference on Decision and Control (CDC)*, pp. 415–420, 2018.
[25] K. Hang, M. Li, J. Stork, Y. Bekiroglu, F. Pokorny, A. Billard, and D. Kragic, "Hierarchical fingertip space: A unified framework for grasp planning and in-hand grasp adaptation," *IEEE Trans. Robot.*, vol. 32, no. 4, pp. 960–972, 2016.
[26] W. Shaw Cortez, D. Oetomo, C. Manzie, and P. Choong, "Control barrier functions for mechanical systems: Theory and application to robotic grasping," *IEEE Trans. Control Syst. Technol.*, vol. 29, no. 2, pp. 530–545.
[27] E. Lavretsky and K. A. Wise, *Robust adaptive control*. Springer, 2013.
[28] M. Mesbahi and E. Magnus, *Graph Theoretic Methods in Multiagent Networks*, ser. Princeton Series in Applied Mathematics. Princeton: Princeton University Press, 2010, vol. 33.
[29] B. Mirtich and J. Canny, "Easily computable optimum grasps in 2-D and 3-D," in *IEEE Int. Conf. on Robot. Autom.*, 1994, pp. 739–747.
[30] W. Shaw Cortez, "Robust Object Manipulation for Fully-Actuated Robotic Hands," Ph.D. dissertation, The University of Melbourne, 2019. [Online]. Available: http://hdl.handle.net/11343/233378
[31] Event-triggered, adaptive control for cooperative manipulation with rolling contacts. [Online]. Available: https://youtu.be/tQcnlBbkAHU
[32] A. Bressan and B. Piccoli, *Introduction to the mathematical theory of control*. American institute of mathematical sciences Springfield, 2007, vol. 1.
[33] H. K. Khalil, *Nonlinear Systems*. Upper Saddle River, N.J. : Prentice Hall, c2002., 2002.
[34] L. Grüne and J. Pannek, *Nonlinear Model Predictive Control*, ser. Communications and Control Engineering. London: Springer, 2017.